
REFLECTIONS

and their impact on production and postproduction of moving images

Bachelorarbeit im Studiengang Audiovisuelle Medien

Hochschule der Medien Stuttgart

vorgelegt von

Amelie Dillig

Matrikelnummer: 23621

Erstprüfer: Prof. Katja Schmid

Zweitprüfer: Peter Ruhrmann

Stuttgart, 05. März 2015

REFLECTIONS

and their impact on production and postproduction of moving images

Bachelor thesis

submitted to the department of Electronic Media

Media University Stuttgart

in partial fulfillment of the requirements for the degree of Bachelor of Engineering

by

Amelie Dillig

Student ID: 23621

Supervision by Prof. Katja Schmid

and Peter Ruhrmann

Stuttgart, March 2015

Eidesstattliche Erklärung

„Hiermit versichere ich, Amelie Dillig, an Eides Statt, dass ich die vorliegende Bachelorarbeit mit dem Titel: „Reflections and their impact on production and postproduction of moving images“ selbstständig und ohne fremde Hilfe verfasst und keine anderen als die angegebenen Hilfsmittel benutzt habe. Die Stellen der Arbeit, die dem Wortlaut oder dem Sinn nach anderen Werken entnommen wurden, sind in jedem Fall unter Angabe der Quelle kenntlich gemacht. Die Arbeit ist noch nicht veröffentlicht oder in anderer Form als Prüfungsleistung vorgelegt worden.

Ich habe die Bedeutung der eidesstattlichen Versicherung und die prüfungsrechtlichen Folgen (§26 Abs. 2 Bachelor-SPO (6 Semester), § 23 Abs. 2 Bachelor-SPO (7 Semester) bzw. § 19 Abs. 2 Master-SPO der HdM) sowie die strafrechtlichen Folgen (gem. § 156 StGB) einer unrichtigen oder unvollständigen eidesstattlichen Versicherung zur Kenntnis genommen.“

Ort, Datum

Unterschrift

Abstract in English

Specular reflections and highlights are significantly characterizing and revealing for the visual perception of surface properties of observed objects.

When capturing moving images, the characteristics of reflections and also refraction are on the one hand often used for effects purposes. On the other hand reflective surfaces partially need to be replaced if they reveal unrequested parts of the surrounding setting, or simulated when it comes to inserting computer generated elements into live-action footage and visual effects. Further, with light field or stereoscopic filming methods, reflections require additional consideration.

This paper delivers insight into the influences of specular reflections on production and postproduction of motion pictures.

Abstract auf Deutsch

Spiegelnde Lichtreflexionen und Glanzlichter sind maßgeblich charakterisierend und aufschlussreich für die visuelle Wahrnehmung der Oberflächeneigenschaften von betrachteten Gegenständen.

Beim Erfassen von Bewegtbildern werden einerseits die Reflexions- und auch Refraktionseigenschaften oftmals für visuelle Effekte genutzt; andererseits müssen reflektierende Oberflächen teilweise ersetzt werden, wenn sie unerwünschte Teile der umgebenden Kulisse preisgeben, oder realistisch nachgebildet werden, wenn es um das Integrieren von computergenerierten Elementen in Realbildaufnahmen und visuellen Effekten geht. Des Weiteren erfordern Reflexionen genauere Betrachtungen bei Lichtfeld und Stereo 3D Aufnahmemethoden.

Diese Arbeit gibt einen Überblick über den Einfluss von spiegelnden Reflexionen auf die Aufnahme und Nachbearbeitung von Bewegtbildern.

Contents

Eidesstattliche Erklärung	i
Abstract in English	ii
Abstract auf Deutsch	ii
1 Introduction	4
1.1 Motivation	5
1.2 Content	5
2 Physical background and basics of optics relating to reflections	6
2.1 Optical principles of reflections	7
2.1.1 Fermat's principle of reflection	7
2.1.2 Snell's law	8
2.1.3 Fresnel equations and polarization	9
2.2 Reflectance characteristics	13
2.2.1 Specular vs. diffuse reflection	13
2.2.2 Specularities and specular reflection	14
2.2.3 Isotropy and anisotropy	16
3 Visual interpretation of reflections	17
3.1 Reflections' impact on visual perception of shape	17
3.1.1 Distortion	17
3.1.2 Motion	18
3.1.3 Intensity	19
3.1.4 Compression	20
3.2 Binocular vision	22
3.2.1 Basics of stereopsis	22
3.2.2 Reflection disparity	24
4 Visual effects with reflections	28
4.1 Use of reflections in the history of visual effects	28
4.1.1 Front screen projection	28
4.1.2 Schüfftan Process	32

4.1.3	Other in-camera effects by means of reflections	35
4.2	Reflections in today's visual effects	37
4.2.1	Boon and bane of reflections	37
4.2.2	Replacement with 2D compositing solution	39
4.2.3	Replacement with CG elements	42
4.2.3.1	Realistic reflection and shading models	42
4.2.3.2	Image-based lighting	48
4.2.3.3	Ray-tracing	51
4.2.3.4	Match moving	55
4.2.3.5	Rendering passes and compositing	57
5	Transferring reflections from the real world to digital 3/2,5D space	60
5.1	Stereoscopy with reflective and glossy surfaces	60
5.1.1	Stereoscopy fundamentals	60
5.1.2	Capturing stereo 3D	63
5.1.3	Problems and irritations related to reflections	65
5.1.3.1	Beam-splitter reflection	65
5.1.3.2	Disparity of reflections	66
5.1.3.3	Reflections and depth	68
5.1.4	Stereoscopic compositing	68
5.2	Light fields and reflective and transparent surfaces	69
5.2.1	Technology of light field camera	69
5.2.2	Problem of glossy surfaces and reflecting objects	72
5.2.3	Approach of solution	72
5.2.3.1	Specular highlights	73
5.2.3.2	Specular and transparent planes	73
5.2.3.3	Refractive objects	74
6	Conclusion and outlook	76
	References	78
	List and References of Figures	82

1 Introduction

Reflections are omnipresent. In fact, our visual experience is based on all kinds of light reflections which are responsible for three-dimensional perception, assist in shape interpretation and reveal new perspectives – without even taken into account that color is also a result of reflection.

Reflection of light is one of the most evident characteristic of light. Besides mirrorlike reflections that we include in our daily life – like the rearview mirror in cars –, there are more subliminal reflections of light that are declared as specular and diffuse reflections.

Especially highly reflective and shiny objects such as sports cars and jewelry can be appealing to look at. However, when it comes to shooting a movie, reflections of the crew and set on reflective surfaces need to be handed on to the postproduction team.

In general, specular reflections and highlights are considered to be more like a nuisance for many aspects of visual processing as they are often very bright features, slide over the surface and change shape whenever the viewer, the environment or the object itself moves. Hence, they tend to cause problems with tracking object motion, setting the right exposure, estimating depth values and stereoscopic images. (cf. Thompson et al., 2011, p. 400) However, both specular and diffuse reflections are very important for the visual system to estimate an object's three-dimensional shape and assist in material perception.

The visual system is perfectly able to interpret all different kinds of reflections in real environment, in moving images and single photographs. Until lately, however, computational systems struggled with interpreting reflections and specular and diffuse highlights as they obscure the structure of the underlying scene. (cf. Blake et al., 1990, p. 165) Thus, it is difficult to analyze and detect the three-dimensional shape of reflecting objects with a computational process.

But although reflections cause many problems, they also offer many amenities for processing moving images. For instance, in the development of visual effects, in-camera techniques like the Schüfftan Process or front projections made use of reflection and refraction properties of different kinds of mirrors. But reflections also affect state of the art production methods like stereo 3D.

Most of the time reflections blend in seamlessly contributing to a scene in terms of depth, shape and material perception. However, if anything is wrong with them, the viewer will certainly doubt an image's authenticity consciously or unconsciously. Therefore, the integrity of reflections in film scenes plays an important role in visual effects and image processing.

1.1 Motivation

In film production and postproduction, reflections play a significant role that requires closer consideration and awareness. The motivation and goal of this work is to analyze, observe and understand the reflection characteristics. The reflections' decisive use, lifelike simulation, coherent replacement and seamless integration – both during producing and post-processing images – should be examined more closely in order to enhance realistic visual results.

1.2 Content

The paper consists of 4 main parts, beginning with the fundamentals of light, the physical principals of reflections and their visible characteristics. Further, the role of reflections for our visual system relating to the perception of shape and binocular vision is examined. A major part of this work deals with reflections and their use in the development of visual effects including in-camera effects, digital compositing and integrating computer generated imagery into live-action footage within the framework of capturing three-dimensional space in flat images. In the last part, the impact of reflections on stereoscopic 3D and light fields is reviewed in context of transferring true three dimensions to digital 3D or rather 2,5D space. Last follows the conclusion and outlook followed by the list of references.

While considering light reflections in this paper, light is referred to as an electromagnetic wave mainly not taking account of the aspect of wavelength and color in particular. Furthermore, the path of rays occurring inside the film camera from the lens system to the sensor is contemplated as preexisting and is thus not reviewed particularly in this work. Therefore, while neglecting the aspect of color, this paper examines the impact of reflections, which occur in front of a camera and “behind” – relating to postproduction.

2 Physical background and basics of optics relating to reflections

Reflections obey the fundamentals of light which is an electromagnetic wave. Visible light consists of a range of wavelengths or frequencies that our eyes respond to. This paper, however, leaves out the aspect of light spectrum and wavelength and consequently color in particular is excluded.

When light strikes a surface, three different types of interaction can occur: reflection, transmission and absorption (Figure 1).

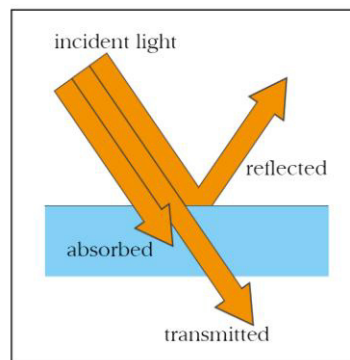


Figure 1: Light interacting with matter.

Reflection is the process in which light is bounced off from the surface of an object. Transmission describes the process when light passes through a medium whereupon its direction may be altered, i.e. refracted. Light that is neither reflected nor transmitted will be absorbed and the light waves' energy usually is converted to heat.

Rarely only one of the cases applies; most of the time, it is a combination of two or all three of these – underlying the law of conservation of energy that states that energy within a system remains constant while it can change from one form to another or transfer from one object to another.

When referring to reflection or reflective objects, it is implied that the majority of the incident rays are reflected but never all of them since a fraction is usually absorbed or transmitted. The same correspondingly applies for transparent and absorbent surfaces.

In this paper, light rays are mostly described as rectilinear paths which are used as an abstraction to simplify how light will propagate and interact with matter. However, there are two different models for the behavior of light: the ray-based model, considering light as particles (photons) traveling through space, and the wave model, describing light as a three dimensional electromagnetic wave including wave effects such as interference and diffraction. Neither the wave-like nor the particle-like model is wrong but particular optical phenomena can be illustrated in a better way with one of the two models.

2.1 Optical principles of reflections

2.1.1 Fermat's principle of reflection

Fermat's principle (1657) states that "light travels between two points along the path that requires the least time, as compared to other nearby paths." (Perrine, 1961)

A ray of light starting at point A reflects off the surface and arrives at point B, as demonstrated in Figure 2. The horizontal distance between A and B is d , as labeled in Figure 2.

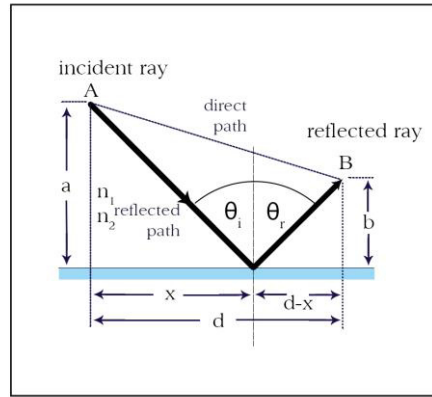


Figure 2: Proof of Fermat's principle of reflection.

With the length of each path the shortest time for the light to travel between A and B can easily be determined by dividing the length by the speed of light.¹ Obviously, the direct path between A and B results in the shortest time, but supposing that the light ray has a given path reflecting off the surface, the path length L from A to B is:

$$L = \sqrt{a^2 + x^2} + \sqrt{b^2 + (d-x)^2}.$$

As the speed of light is constant, the shortest time path is the shortest distance path. In order to minimize the path traveled by light, the first derivative of L – with respect to x – is taken and set to 0. (cf. Nave, 2012)

$$\frac{dL}{dx} = \frac{1}{2} \frac{2x}{\sqrt{a^2 + x^2}} + \frac{1}{2} \frac{2(d-x)(-1)}{\sqrt{b^2 + (d-x)^2}} = 0$$

This can be reduced to:

$$\frac{x}{\sqrt{a^2 + x^2}} = \frac{(d-x)}{\sqrt{b^2 + (d-x)^2}},$$

¹ $t = \frac{d}{c}$, with t as the time and c as the speed of light.

which leads according to the definition of sine to:

$$\sin \theta_i = \sin \theta_r,$$

and therefore results:

$$\theta_i = \theta_r.$$

Referring to Figure 2, when a light ray strikes a surface making an angle of incidence θ_i with the surface normal (the perpendicular to the surface), it is reflected at the same angle of reflection θ_r with the surface normal. Additionally, the incident and reflected light rays lie on the same plane named plane of reflection. These two properties mark the law of reflection.

This is a fundamental law of optics from which other laws of geometrical optics like the Law of Reflection and Snell's law can be derived.

2.1.2 Snell's law

Snell's law of refraction can also be deduced from Fermat's principle that further says that when light travels from a point in an optically rare medium with a given light velocity to a point in an optically denser medium, in which the light travels slower, or vice versa, the light takes such a path as to make the journey in the least possible time. (cf. Myers, 2006, p. 151f)

When light enters a denser or rarer medium, it bends according to Fermat. (cf. *ibid.*) This amount of bending or refraction can be estimated by Snell's Law. As shown in Figure 3, a ray travelling in a medium n_1 with an angle of incidence θ_1 is transmitted into a medium n_2 with an angle of refraction θ_2 with respect to the surface normal; n_1 and n_2 are the medium specific indices of refraction. (cf. Hecht, 2002, chap. 4, 5)

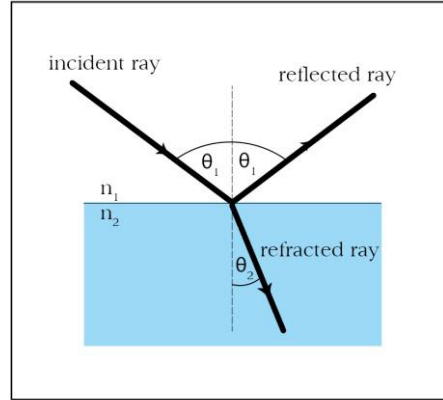


Figure 3: The law of refraction.

The relation between the two angles θ_1 and θ_2 for any two different dielectric² media with indices of refraction n_1 and n_2 is defined in Snell's Law as:

$$n_1 \sin \theta_1 = n_2 \sin \theta_2$$

2.1.3 Fresnel equations and polarization

Another fundamental in optics are the Fresnel equations derived by Augustin-Jean Fresnel based on Snell's Law, in 1832. These Fresnel equations relate the amplitudes, phases and polarization of transmitted and reflected light waves when light arrives at an interface between two transparent media with different refraction indices. (cf. Lvovsky, 2013, p. 1)

The equations induce the polarization of light waves. Light waves have an electric (and magnetic field), which is vibrating in time and space. If the electric field of a light ray vibrates in a constant plane in space, it is referred to as linear polarized light. Fresnel's equations consider two cases of polarization: polarization parallel to the incident plane, referred to as p-polarization, or perpendicular to the incident plane s-polarization, which relates to light as a three-dimensional wave with a certain polarization, i.e. orientation as demonstrated in Figure 4.

² A dielectric medium can sustain an electric field within it but does not conduct electricity. (cf. Allaby et al., 1999)

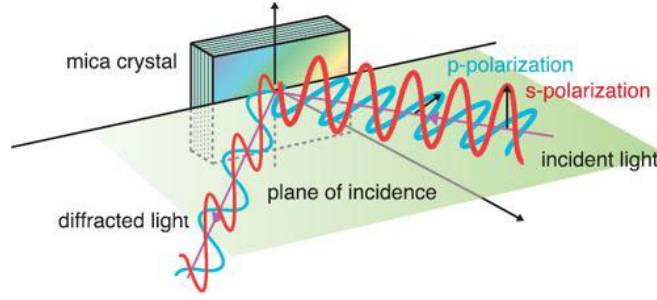


Figure 4: Parallel (p-) and perpendicular (s-) polarization to the plane of incidence.

The Fresnel equations correspond to the reflection coefficients r_p , r_s and transmission coefficients t_p , t_s – each considering parallel and perpendicular polarization. The reflection coefficients describe the ratio of the reflected electric field amplitude of the light wave to the incident one. Correspondingly, the transmission coefficients describe the ratio of the transmitted electric field amplitude of the wave to that of the incident wave.

Fresnel equations for parallel, i.e. p-polarized light:

$$r_p = \frac{(n_2 \cos \theta_1 - n_1 \cos \theta_2)}{(n_1 \cos \theta_2 + n_2 \cos \theta_1)}$$

$$t_p = \frac{2n_1 \cos \theta_1}{(n_1 \cos \theta_2 + n_2 \cos \theta_1)}$$

Fresnel equations for perpendicularly, i.e. s-polarized light:

$$r_s = \frac{(n_1 \cos \theta_1 - n_2 \cos \theta_2)}{(n_1 \cos \theta_1 + n_2 \cos \theta_2)}$$

$$t_s = \frac{2n_1 \cos \theta_1}{(n_1 \cos \theta_1 + n_2 \cos \theta_2)}$$

Again, referring to Figure 3, n_1 and n_2 are the refractive indices of the two dielectric media, θ_2 is the refraction angle and θ_1 is the angle of reflection, which is equal to the angle of incidence towards the surface normal, according to the law of reflection (chapter 2.1.1).

However, for practical purposes, the fraction of the intensity, i.e. power, being reflected and transmitted from the interface is more of interest. It is given by reflectance or reflectivity R for the reflected fraction and transmittance T for the refracted fraction as the square of the reflection coefficient r and transmission coefficient t . (cf. *ibid.*, p. 2)

Reflectance for parallel, i.e. p-polarized light:

$$R_p = \left(\frac{(n_2 \cos \theta_1 - n_1 \cos \theta_2)}{(n_1 \cos \theta_2 + n_2 \cos \theta_1)} \right)^2$$

Reflectance for perpendicular, i.e. s-polarized light:

$$R_s = \left(\frac{(n_1 \cos \theta_1 - n_2 \cos \theta_2)}{(n_1 \cos \theta_1 + n_2 \cos \theta_2)} \right)^2$$

In consequence of the conservation of energy, the fraction of transmittance T can easily be calculated as a difference but not as the square of t . (cf. *ibid.*, p. 3) The minor absorption at the interface is neglected.

Transmittance for parallel, i.e. p-polarized light:

$$T_p = 1 - R_p$$

Transmittance for perpendicular, i.e. s-polarized light:

$$T_s = 1 - R_s$$

On the left in Figure 5, a graph of the reflectance intensity R_p and R_s is shown as a function of the incident angle at an interface of air (n_1) and glass (n_2) with $n_1 < n_2$. According to this graph, at normal incidence ($\theta_i = 0^\circ$), perpendicularly and parallel polarized light waves have the same reflectivity of about 4 % and are not distinguishable. (cf. *ibid.*) With increasing angle of incidence, more and more light is reflected and at $\theta_i = 90^\circ$ 100 % is reflected, which means that the interface acts as a mirror.

The graph on the left also exhibits that the reflectance is 0 for parallel polarized light at an incidence angle of $\theta_i = 56.3^\circ$, which is referred to as “Brewster’s angle”.³ At this special angle, light having its polarization axis in the plane of incidence is fully transmitted. Thus, only perpendicularly polarized light is reflected, as demonstrated on the right.

The reflected light and the refracted light are 90° apart when the angle of incidence is set at Brewster’s angle, which depends on the refractive indices of the two media.

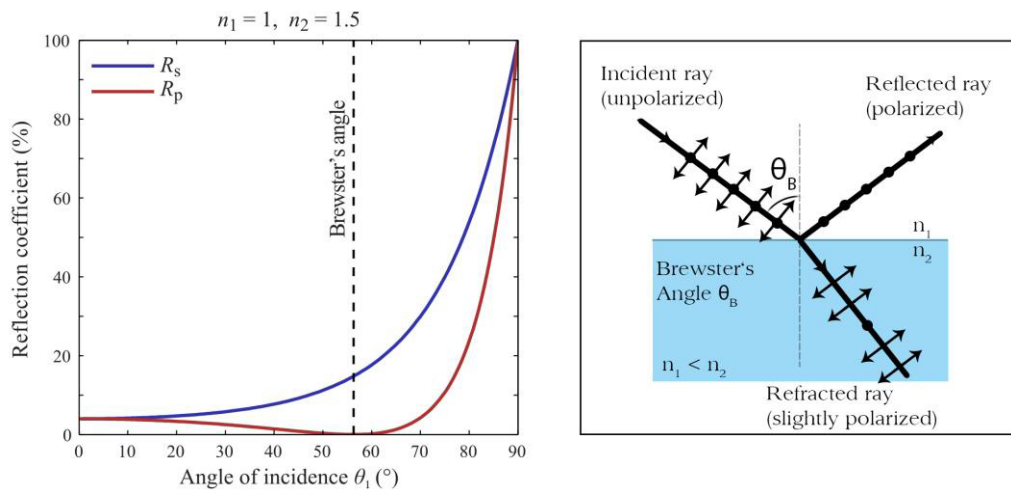


Figure 5: Left: Reflectance R_s and R_p at an air-glass interface. Right: Brewster’s Angle.

³ It is named after the Scottish physicist Sir David Brewster (1781-1868).

⁴ Complex numbers consist of a real part and an imaginary part.

Accordingly, a disproportionate part of the reflected light tracing towards the viewer or camera sensor is linearly polarized. By using a polarizing filter, linearly polarized light waves can be eliminated and therefore reduce reflections and disturbing glare.

The graph on the left in Figure 6 shows the reflectance intensity R_p and R_s as a function of the incident angle at an interface of glass (n_1) and air (n_2) with $n_1 > n_2$. According to this graph, at normal incidence ($\theta_1 = 0^\circ$), again about 4 % of the light waves are transmitted and are not distinguishable in terms of polarization. With increasing angle of incidence, the angle of refraction rises until the so called critical angle. For incident angles θ_1 less than the critical angle, a part of the incident light waves is reflected and a part of them is transmitted, as shown on the right of Figure 6. By setting the refraction angle equal to 90° , the critical angle can be calculated from Snell's Law, so that:

$$\sin \theta_c = \frac{n_2}{n_1}.$$

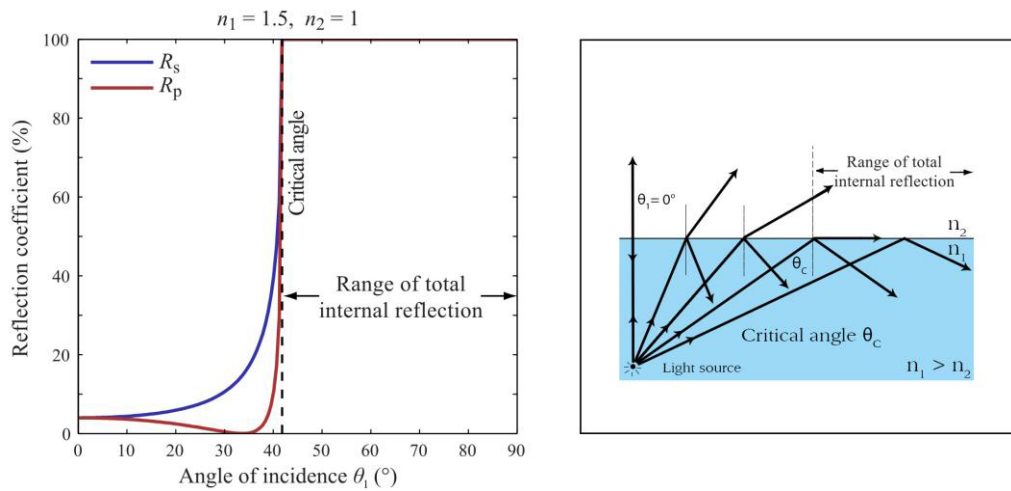


Figure 6: Left: R_s and R_p at a glass-air interface. Right: Critical angle and total internal reflection.

As exhibited in Figure 6, when light strikes a medium with a lower refraction index with an incident angle above the critical angle, it is totally reflected. Then, no light from the light source leaves the medium n_1 and all light waves are reflected, which leads to the term total internal reflection. For both p- and s-polarized light waves above the critical angle, the light source is not visible at corresponding viewpoints in n_2 .

These Fresnel equations approximately apply to most dielectric materials, such as glass and water. However, for absorbing materials and metals, which have a complex⁴ index of

⁴ Complex numbers consist of a real part and an imaginary part.

refraction, the formula needs to be expanded and there is neither a Brewster angle nor refracted light.

In general, as light is an electromagnetic wave it exhibits polarization. Sunlight and light from most light sources is unpolarized. The light's electromagnetic fields can also be orientated in a single direction, referred to as linear polarization, or rotate, which is referred to as circular or elliptical polarization, with either clockwise or counter clockwise direction. Light can be partially polarized by reflecting on a surface and also by scattering off the molecules of the atmosphere, which is responsible for the blue sky. Polarization filter can eliminate light waves with a specific orientation.

2.2 Reflectance characteristics

2.2.1 Specular vs. diffuse reflection

In general there are two forms of reflection. One is specular reflection in which parallel rays are reflected at the same angle at each point, according to the law of reflection, as demonstrated in Figure 7 (left). The surface then usually looks shiny and the incoming light rays bounce off the surface so that a reflection of the light source itself can actually be seen on the surface. The other form of reflection is diffuse scattering or reflection in which light rays are reflected unpredictably in many directions, as shown in Figure 7 (right).

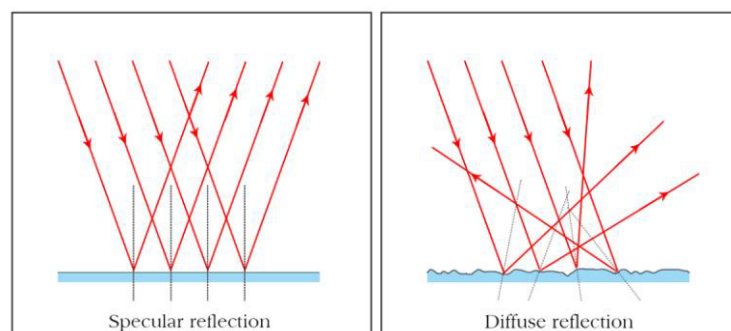


Figure 7: Types of reflection.

Comparing a smooth, glossy surface to a surface that is rough or dull, the difference can clearly be noticed. A glossy surface appears brighter as the parallel reflected rays are aligned; whereas a diffuse surface appears dimmer as rays are reflected in random

directions, e.g. the green felt of a pool table. (cf. Myers, 2006, p. 152) As a result, only a small part of the incoming light rays actually make it to our eyes or the sensor of a camera, so that diffuse surfaces appear much dimmer than the light sources that illuminate them. The exposure for capturing a scene is based on the brightness values of the diffuse surfaces; specular reflections that reflect the actual light source are usually so bright that they get clipped as. (cf. Wright, 2010, p. 203f)

In fact, the vast majority of the captured objects found in a typical movie sequence have diffuse surfaces, as they make up what we think of as the "common" dull surfaces such as clothes, skin, furniture, trees and the ground. (cf. Wright, 2010, p. 203f) However, the more challenging part for image processing derives from the reflecting surfaces found in a scene, which are plenty enough.

2.2.2 Specularities and specular reflection

Flat or undulating semi specular surfaces create luminance highlights, which are usually reflections of light sources. These are referred to as specularities or specular highlights, illustrated in Figure 8 (right). (cf. Howard et al., 2012)

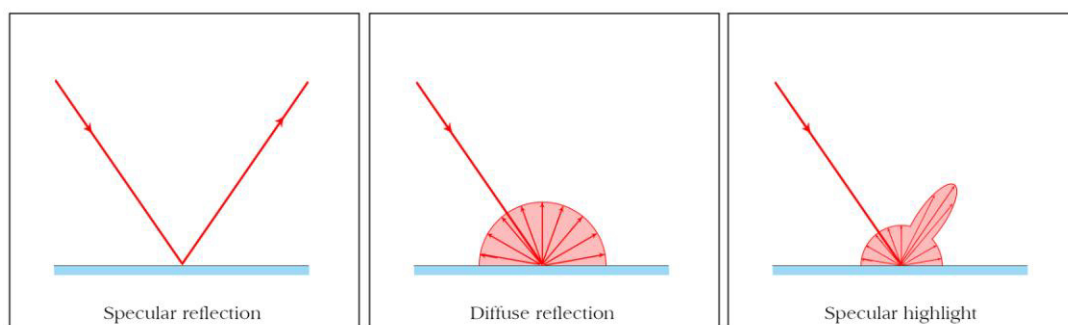


Figure 8: Materials have different reflectance properties.

The size of specular highlights depends of the smoothness and shape of the object. A polished billiard ball will have a smaller, brighter highlight than a rubber ball, which will have a larger fuzzier one.

Another key property of both specularities and specular reflections is that their colour is usually based more on the light source's colour than on surface's colour. This varies to a large extent with materials, of course. For example glass and chrome largely reflect the true colour of the light source. However, copper tints the reflections to reddish colour. The conclusion here is that specularities and specular reflections cannot be taken as a

reference for the colour of a surface, due to the fact that it depends very much on the colour of the light source being reflected.

Same as the colour, the location of the specularities also depends a lot on the position of the light source. Both specular reflections and specular highlights move along with even slight changes in position of the light source, orientation of the surface or the location of the camera or viewer referring to Figure 9 (right). They are not fixed on the surface like texture markings but slide over the surface and change shape whenever there is a change in position of the light source, environment or viewpoint.

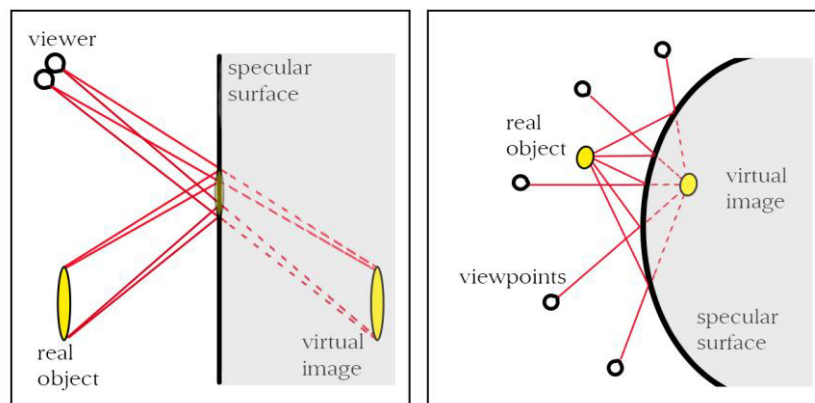


Figure 9: The virtual image appears to be the same distance behind the specular surface as the object is in front of it.

As shown in Figure 9, the position of a reflection can be estimated by considering a virtual image lying behind the reflecting surface. The virtual image is formed in a position where no light actually reaches it; it only appears to the observer that the light comes from a location at the other side of the mirror.

Based on the virtual image, the location of the reflected image or specularities can easily be estimated depending on the viewer's position.

While the location of specular reflections, same as specular and glossy highlights, depends on the viewer's position, diffuse reflections' location is mostly independent of the observer's position.

2.2.3 Isotropy and anisotropy

So far, only isotropic⁵ materials, i.e. materials with identical properties independent of direction, have been considered. Isotropic materials distribute reflections evenly in all directions on a surface. However, there are materials which differ with orientation, thus, are directionally dependant, referred to as anisotropic⁶ property. Such materials exhibit significantly different reflection characteristics.

In isotropic materials microscopic roughness, which is responsible for diffusing light, is distributed randomly. In contrast, the structure of anisotropic materials has small grain or grooves which are distorted and stretched in one or more orientations.

Examples for anisotropic surfaces are hair, CDs, brushed metal, velvet, feathers, etc. As shown in Figure 10, anisotropic reflections and highlights are stretched perpendicularly to the direction of the grooves or grain of the surface. (cf. Birn, 2000, p. 199)



Figure 10: Anisotropic reflections on hair and brushed metal.

⁵ Isotropic means identical in all directions. (cf. Allaby et al., 1999)

⁶ Anisotropic means that properties vary according to the direction of measurement. (cf. *ibid.*)

3 Visual interpretation of reflections

3.1 Reflections' impact on visual perception of shape

Estimating the three-dimensional shape of an object based on the reflections on its surface is an astonishing and perplexing ability of the visual system.⁷

When an object moves in three dimensional space, the appearance can change drastically. We can interpret a reflective object's shape even though the reflections on the surface continuously change just because the shape itself still appears stable. (cf. Fleming et al., 2004, p. 799) In fact, specular surfaces adopt their appearance solely from their surroundings as almost every visible feature belongs to the environment surrounding the object rather than to the object itself (cf. Figure 11).



Figure 11: The surface of a reflective object changes utterly when varied in position.

This leads to the question how the visual system extracts relevant information of the reflection to constrain shape and surface properties. Another question is whether our brain knows the physics of specular reflections. (cf. Fleming et al., 2004, p. 800) The following sections will look into these questions.

3.1.1 Distortion

To infer shape from given reflections, the visual system first locates and recognizes the distortion of the reflection on the surface of an object, e.g. a rectangle which is warped into a wedge shape, shown in Figure 12 (left). Secondly, the visual system estimates the

⁷ The visual system of humans includes communication between the eyes and the brain that interprets given stimuli as images.

deforming transformation that the surface geometry applies to the shape of the reflection. As soon as the visual system knows the transformation of the deformation, it is able to recover the surface's three-dimensional shape that provokes the distortion. As an example, if a reflection shows curved lines while the corresponding real feature are straight lines, the visual system can estimate the three-dimensional curvature of the specular surface by considering the degree of curvature in the reflection, as shown in Figure 12 (right). (cf. *ibid.*, p. 800)

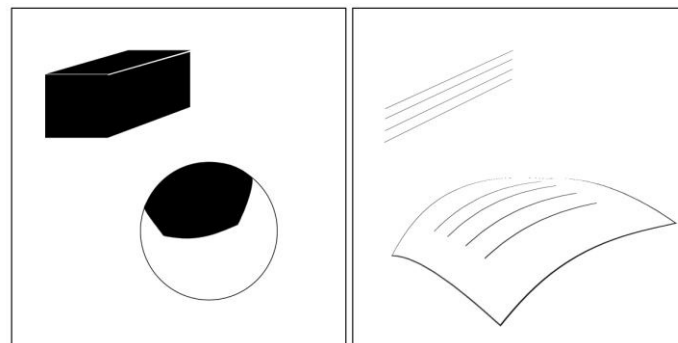


Figure 12: Recovering shape by analyzing the distortion.

However, this way of recognizing a surface's shape is based on the knowledge of the undistorted feature in the surrounding environment. Thus, the visual system can only interpret the reflected image if it receives information about the surroundings or makes assumptions about the surrounding features, e.g. lines are usually straight. (cf. *ibid.*, p. 800)

3.1.2 Motion

In addition, more information about an object's shape can be deduced from the property that specular reflections depend on the viewer's location. In comparison to texture and diffuse reflections, which are view independent, specular highlights and reflections move relative to the surface whenever the viewer or the object changes position. Thus, motion on a surface is needed to be able to distinguish between diffuse surface markings and specularities.

Further, the specific behavior of the specularities' motion gives hints about the curvature of an object. Specular highlights slide faster across surface regions of low curvature and move slower across surface regions of high curvature. (cf. Koenderink et al., 1980) Another characteristic of specular movement is that it corresponds with the viewer's movement on a convex surface, whereas it is opposite to the viewer's movement on a

concave surface. (cf. Zisserman et al., 1989, p. 39) This feature can be observed on the concave and convex side of a spoon. Referring to this property of specularities, the visual system gauges whether a surface is convex or concave.

3.1.3 Intensity

Despite the visual system's interpretation of the motion and velocity of the specularities, it can also recognize reflective surfaces in static images. An important source of information is conveyed by specular highlights. Highlights are principally brighter than diffuse surface markings as the reflection on the surface is more focused. The visual system can use this outstanding intensity of a feature in the image as a cue to distinguish a highlight from diffuse surface markings or texture, as demonstrated in Figure 13 in the upper row. (cf. Fleming et al., 2004, p. 799)



Figure 13: Surface perception changes when intensity of highlights changes.

In fact, the visual system expects highlights to be at least as bright as their surroundings. As shown in Figure 13 in the lower row, the perception of a surface changes significantly when the specular highlights in an image are removed. The surface rather looks matte and diffuse and does not appear glossy, wet or polished any more. (cf. Thompson et al., 2011) Thus, the intensity of specularities can also allow the visual system to draw conclusions about surface characteristics, such as glossiness, and to detect specular highlights in static images.

3.1.4 Compression

Surface textures exhibit a different pattern of compression than specular reflections. This feature allows distinguishing between texture and reflection. (cf. Fleming et al., 2004, p. 804) Figure 14 shows a planar surface being rotated in depth. In the left column, the surface consists of an isotropic texture. In the right column, the surface is a perfect mirror.

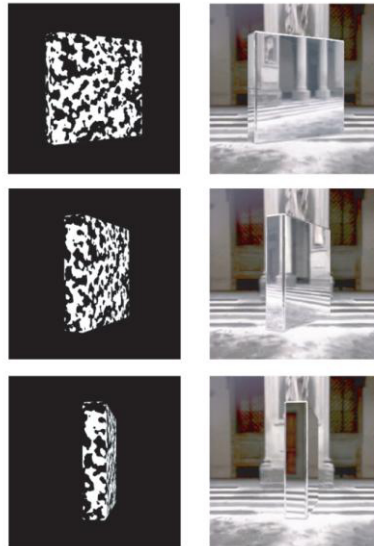


Figure 14: Comparison of a textured surface on the left column and a mirror on the right.

As the textured surface gets rotated away, as seen in Figure 14, it becomes more and more compressed because of foreshortening. However, when the mirror surface gets rotated away, the mirror reflects different parts of the surroundings but the reflection is not compressed at all, demonstrated in Figure 15. (cf. *ibid.*)

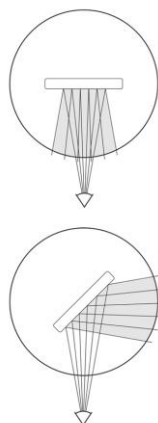


Figure 15: There is no compression of the reflection when a planar mirrorlike surface is rotated away from the viewer.

In Figure 16 the behavior of compression for curved surfaces is pictured comparing a textured surface in the left column and a mirror surface in the right column.

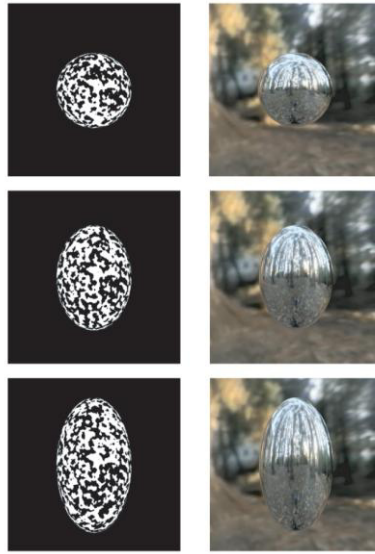


Figure 16: A sphere stretched to an egg shape – with textured surface in the left column and mirror surface in the right column.

The upper image pair shows that towards the edge of the textured sphere, the texture is slightly compressed; in the case of the mirror, there is also a compression of the reflected image. The reason of the compression on the mirrorlike surface is of different origin though. As Figure 17 shows, a highly curved, reflective surface pictures more of the surroundings than a slightly curved one. (cf. *ibid.*, p. 805)

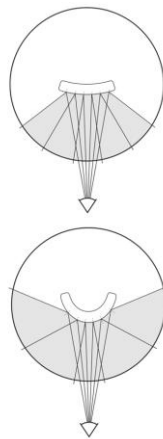


Figure 17: The more curved the surface, the higher the range of reflection.

Hence, a higher curvature compresses the reflection of the surrounding into a small portion of the surface. So, the more the surface is curved, the greater the compression is. (cf. *ibid.*, p. 805)

In case of the textured surface, when the sphere is elongated into an oval shape, more texture elements are sampled on the surface and there is slightly less compression along the vertical axis of the egg. In the case of the mirrored surface, this effect is more dramatic. In the direction of high curvature, a large angle from the surrounding world is compressed into a small portion in the reflected image. Unlike in the direction of low curvature, only a few features from the surrounding world are compressed into a relatively large area of the image. In fact, in regions of minimum curvature the reflected image is stretched into parallel streaks. (cf. *ibid.*, p. 805)

Summing up, textures are compressed along directions of high slant, whereas reflections are compressed along directions of high curvature. This different mapping can be used by the visual system to distinguish between textures and specular reflections.

Another component that needs to be considered to answer the questions of whether our brain knows the physics of specular reflections and how it interprets specular reflections and depth, is binocular vision, which is explained in the following chapter.

3.2 Binocular vision

3.2.1 Basics of stereopsis

Vision where creatures use two eyes simultaneously is referred to as binocular vision. Due to the different position of each eye – average adult's eye distance is 6,5 cm – binocular vision creates two slightly different images of the environment, referred to as binocular disparity. This binocular disparity provides information, which the brain uses to determine depth of seen objects. This phenomenon is responsible for major means of depth perception. The impression of depth perceiving with binocular viewing is designated stereopsis.

Each eye provides approximately a 130-degree field of view. Combining the images together, a nearly 180-degree field of view is achieved. This results in the so-called Cyclopean image: the single mental picture that a Cyclops can see and which the brain creates by combining the different images of the two eyes. Unlike horses or chameleons, humans' eyes are located side-by-side, which allows overlapping of the two images. The brain developed a mechanism to fuse the two slightly different images to one by matching up similarities. In fact, the fused picture is more than the sum of its parts. It is a three-

dimensional image with depth information. However, fusion of two images without double vision (diplopia), occurs only in a small volume of visual space. This area is around the eyes' fixation point for which objects fall on corresponding points on the eyes' retina. These are the so-called corresponding retinal points, which provoke single vision (Figure 18). (cf. Kalloniatis et al., 2007)

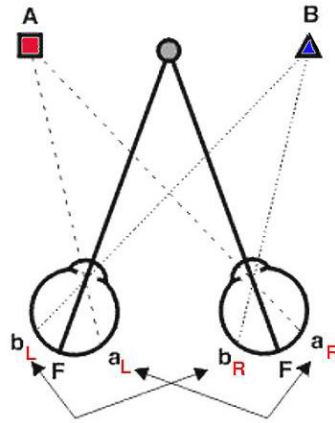


Figure 18: a_L and a_R as well as b_L and b_R are corresponding retinal points.

For objects closer or further away than the fixated point, diplopia occurs arising from the stimulation of non-corresponding retinal points as shown in Figure 19.

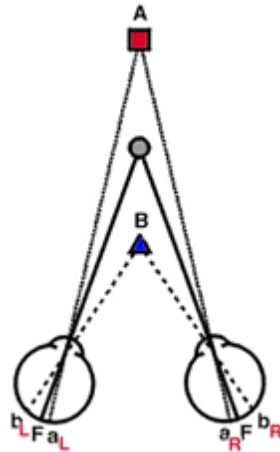


Figure 19: While the grey dot is the eyes' fixation point, A and B stimulate non-corresponding retinal points leading to double vision.

For objects closer to the fixation point, it is called crossed diplopia; for objects more distant to the fixation point it is named uncrossed diplopia.

The points at the same distance as the fixation point form the so-called horopter.

The multitude of points in three-dimensional space, which stimulates corresponding retinal points in the two eyes, is called Panum's fusional area. (cf. *ibid.*) Outside the Panum's fusional area double vision occurs, as illustrated in Figure 20. However, this

diplopia is suppressed by our visual system and hence, double vision is usually not noticed. (cf. *ibid.*)

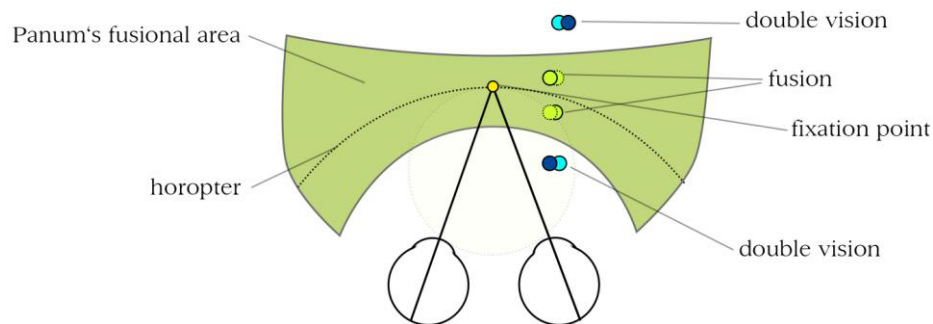


Figure 20: Panum's fusional area spreads around the horopter including fixation point.

Binocular rivalry occurs when the two eyes' images are significantly different from one another. Then, one eye's view dominates for a short period of time, i.e. a few seconds, and is relieved by the image of the other eye afterwards. Thus, besides diplopia, binocular rivalry is another special case of suppression, in which the brain switches from one dominant perspective to the other eye's perspective. (cf. Heeger, 2006)

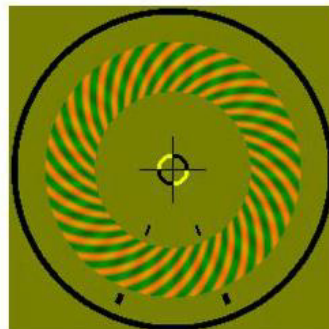


Figure 21: Horizontal grating presented to one eye continuously changing to vertical grating perceived by the other eye.

Referring to Figure 21, the visual system does not have conscious impact over the percept; force of will cannot change the percept to switch. (cf. *ibid.*) This phenomenon is referred to as binocular rivalry.

3.2.2 Reflection disparity

As illustrated in chapter 0, the position of reflections on a specular surface depends on the viewpoint of the observer. This fact becomes important when viewing with two eyes. This means that when a specular surface is viewed binocularly, i.e. from two viewpoints at the same time, corresponding reflections fall on different surface locations, vary in shape or possibly appear only on one eye's image.

Binocular vision provides a source of information about the depth structure of a surrounding environment. To infer depth from binocular disparities, the visual system matches image features between the two eyes' views. For diffuse objects, elements that match between the eyes' perspectives usually have a similar form and appear at corresponding retinal points (cf. chapter 3.2.1). (cf. Murry et al., 2014)

However, glossy objects cause binocular disparity signals, which are quite different to disparity signals from diffuse objects. Due to the different location of the eyes, a single light source is reflected from different surface points. (cf. *ibid.*)

Thus, as illustrated in Figure 22, the specular reflection of the light source appears in front of a concave surface, but behind a convex surface.

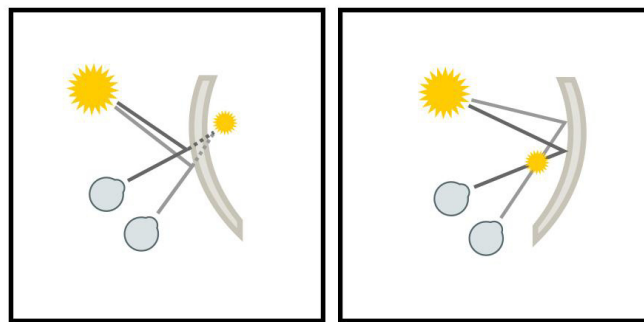


Figure 22: Specularities lie behind convex surfaces (left), but in front of concave surfaces (right).

As a result, specular highlights are located at a position in three-dimensional space that is different from the surface of the reflecting object. (cf. Kerrigan et al., 2013)

Light irradiating from all different directions and matching vectors of reflected rays will mark the virtual surface (referring to Figure 23). This depth difference between the virtual surface and the physical surface location is a challenge to the visual system.

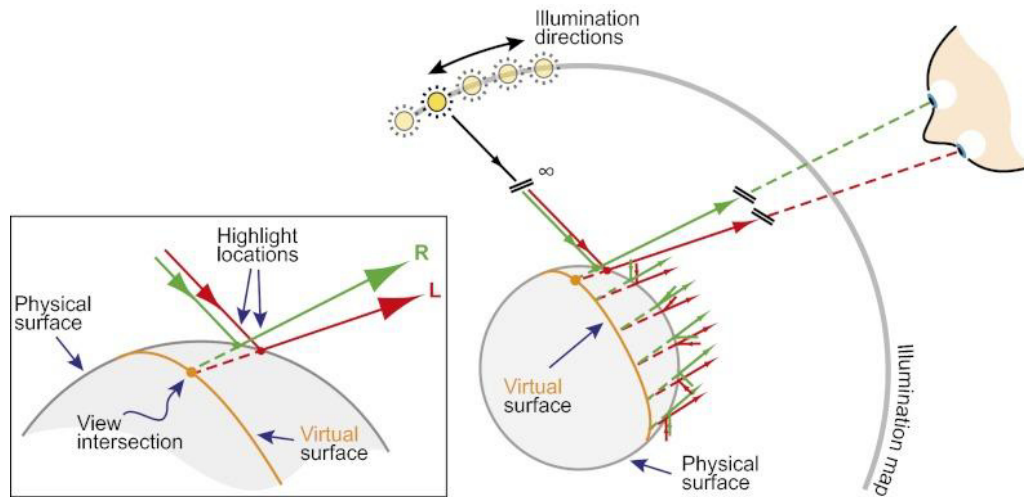


Figure 23: Disparity of highlight position in binocular vision.

After all, for the visual system highlight disparity is a strong factor for the perception of gloss and leads to material authenticity. (cf. Blake et al., 1990, p. 165f), (cf. Wendt et al., 2008, p. 1) A key component for the specific appearance of highlights seems to be binocular rivalry, as explained in chapter 3.2.1. Here binocular rivalry means that even when accounting for binocular disparity and fusing the two images, the resulting luminance does not match in both eyes' images. (cf. Templin et al., 2012, p. 1)

Getting back to the preceding questions: In previous work, Blake and Bülthoff suggested that the human visual system may employ the physics of specular reflection (cf. Blake et al., 1990, p. 165) which implies that it might be capable to reconstruct depth from reflective surfaces and to use the reflections' locations to determine surface material characteristics. However, in recent work, Murry et al. suggest that rather than knowing the physics of specular reflection, the majority of irritations and problems that the visual system faces when observing specular surfaces, may “result from the nature of the disparity signals themselves.” (Murry et al., 2014) In particular, they suggest that the visual system treats the horizontal components of disparity (related to the different horizontal position of the eyes) as indicator of depth, while the orthogonal components may be concerned “as an indicator of the reliability of the depth estimate signal.” (ibid.) This means that where image regions are unmatchable, no depth estimate results, whereas in regions with matching locations, the visual system treats the depth estimates at face value, leading to depth signals that correspond to the virtual image, i.e. the reflections, rather than the physical surface itself. (cf. ibid.)

As explicated in this chapter, it can be assumed that the visual perception of reflections is a complex issue, which has not been fully understood and is yet to be investigated further.

Nonetheless, it is important to analyze and simulate the behavior and properties of specularities and specular reflections to be able to create digital images containing reflections when it comes to visual effects, computer generated imagery and stereo 3D film which is expounded in the following chapters.

4 Visual effects with reflections

4.1 Use of reflections in the history of visual effects

Decades ago, before the technique of green and blue screen was established, cinematographers started experimenting with combining different components in-camera. Mirrors – making use of the reflection properties – were a common tool for creating different layers of action.

4.1.1 Front screen projection

Front screen projection is an in-camera special effect that combines foreground performance with pre-filmed background footage. It allows scenes to be projected to a highly reflective screen behind the actors performing on the studio set in front. Due to the 3M company's development (or at least the selling) of a retro-reflective screen, which goes by the name Scotchlite, the method of front projection came to fruition. (cf. Davidhazy, 2008)

The actor performs in front of the Scotchlite screen or alike with the camera pointing straight towards him. With a set-up as shown in Figure 24, where the projected footage is first reflected on the two-way mirror angled at 45° between both projector and camera, and then onto the actor and the screen, the actor appears to be on the set of the pre-filmed material.

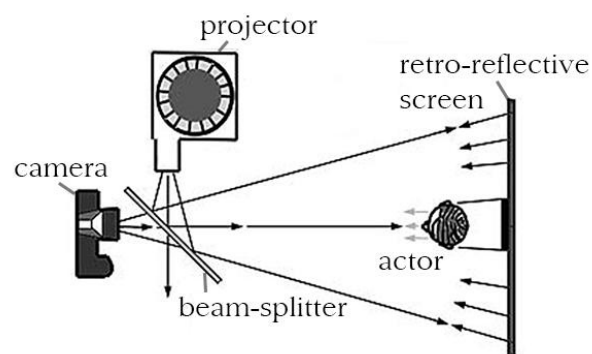


Figure 24: Front projection technique.

Projector and camera lens are aligned so that their axes are coincident.

Now, the obvious question, why the projected image is not at least partially visible on the actor in the foreground – especially as the real action is much closer to the camera than the projection which bounces off the highly reflective screen in the background – comes up.

The answer derives from the fact that the scene's exposure must be adjusted to the bright reflected image in the background, which is around 100 times brighter than the foreground action, due to the strong reflectivity properties of such materials as Scotchlite. The performer would still be seen as a dark silhouette against the brilliant background, even if the person wore a silver suit or was lit by an enormous amount of light. Even though on set it might be possible to slightly see the projected image upon the actor in the foreground, it would be impossible for a camera to capture, as there is no emulsion or sensor with such wide latitude to cope with the huge brightness contrast range. If it was possible to bring up such a huge amount of light to balance the foreground with the immensely bright background reflected from the screen, this light would certainly eclipse any residue of the projected image falling onto the subject in the foreground. (cf. Lightman, 1968)

It is an important requirement of front screen projection that the camera and projector are aligned precisely, that the projector of the light source and the camera are actually positioned at the same spot – in other words, as if the projector was inside the camera. Otherwise, the matte, which the actor himself draws behind him on the screen, would not be coinciding and a shadow of the actor or the subject would be visible, because the screen reflects the projected light directly back to its source. This is due to the unidirectional reflectivity of the screen material that is used. (cf. *ibid.*)

Retro-reflective material such as Scotchlite reflects the incident light back to its source. It uses the three core principles of retro-reflection: Specular reflection, like from a mirrorlike or polished surface as referred to in chapter 2.1.1, refraction, the change in direction of light as it passes from one medium to another with different refraction indices (cf. chapter 2.1.2), and the total internal reflection, saying that where light strikes a transparent surface at a certain angle, it bounces off the surface rather than passing through it. (cf. Lloyd, 2008, p. 1) There are two different systems of retro-reflectivity – one based on glass beads and one with prismatic reflectors. The more common one is the one with glass spheres, where the incident light ray is refracted as it passes through the front surface of the glass sphere and is reflected off a mirrored surface at the back of the bead.

Then the light ray passes back through the front surface, is then again refracted leaving the sphere and thus returns towards the light source in the same direction, as Figure 25 shows.

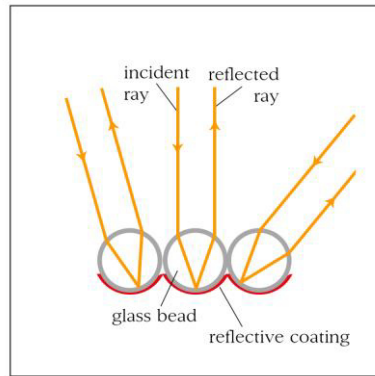


Figure 25: Glass beads retro-reflecting light rays.

Depending on the indices of refraction, different types of beads cause different amounts of light to be retro-reflected towards the light source. Screens used for front projection usually consist of millions of glass beads, each no bigger than 0.4 mm, aligned at the reflective surface. (cf. *ibid.*, p. 2)

These very small glass beads were also used on cinema screens to make them brighter. Scotchlite is also used in highway signs so that they appear very bright and serve like a light source to drivers as they are close to the light source's location of the car. While a simply white painted sign that only reflects back around 50 % of the incident light, Scotchlite reflects back more than 95 % to the light source. (cf. Davidhazy, 2008)

The other core optical component of the front projection technique is the two-way mirror or beam-splitter, which splits an incident light beam into two (or more). And vice versa, beam-splitters also fuse two different light rays into one when used reversely. Among the various existing types of beam-splitters, the cube beam-splitter is the most common one used for front projection method. It is composed of two right-angle prisms, which are agglutinated and thus form a cube, as demonstrated in Figure 26. One prism's hypotenuse surface is covered with coating. The absorption in the special reflective coating is very low so that the reflected part and transmitted part approximate 50 % each, which leads to the desired half reflecting, half pass-through mirror. (cf. Center for Occupational Research and Development, 1987)

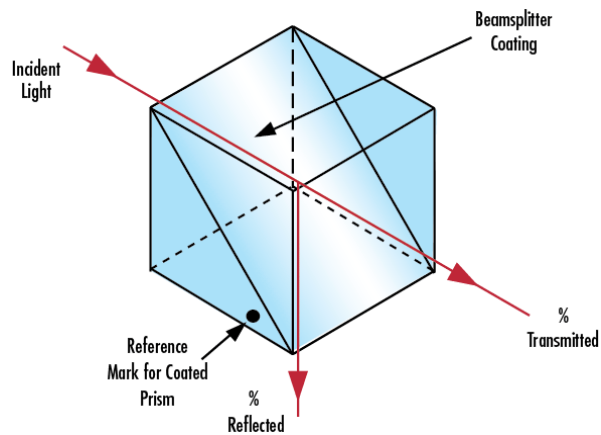


Figure 26: Beam-splitter cube, which can be polarizing or non-polarizing.

Because green and blue screens are so easily and commonly used in today's visual effects productions, the first method filmmakers think of to realize their visual effects ideas, is not front screen projection. However, not only in the beginning of visual effects in the middle of the 20th century but also in the today's blooming visual effects industry, some true masterpieces have been produced with the aid of front projection. Certainly one of the best examples for front screen projection in the history of special effects is Stanley Kubrick's "Dawn of Man" scene in "2001: A Space Odyssey" created in the late 1960s.



Figure 27: Front screen projection in the "Dawn of Man" scene.

Kubrick brought front screen projection to perfection but it was actually Will F. Jenkins who invented the method of front projection that he patented in 1955. (cf. Stallings et al., 2011, p. 137)

A further development of front projection is introvision, which uses a second screen facing the beam-splitter, i.e. the projector and the camera. In the front screen projection described above, light travelling from the projector through the beam-splitter ends to 50 % unused opposite of the projector. In introvision, another retro-reflective screen placed at opposite of the projector bounces the image back towards another Scotchlite screen placed in front of the actor. Parts of this screen can be masked off with black masks. So

actually the same image appears from two different light sources and falls onto two different screens with different depth levels. By having foreground, background and the performance in the midground, introvision can thus place actors in a more realistic three-dimensional environment. (cf. Sfetcu, 2011) It was first applied in 1981 in “Outland” starring Sean Connery, then in e.g. “Under Siege”, “Army of Darkness” and “The Fugitive” (1993), where Harrison Ford seemed to be placed on a bus while a train crashes into it, as shown in Figure 28. (cf. *ibid.*)



Figure 28: Introvision used in the train crash scene in “The Fugitive”.

4.1.2 Schüfftan Process

Eugen Schüfftan, a German Jew cinematographer, invented the so called Schüfftan process which is an in-camera special effect allowing live action to be inserted into a miniature set. In the late 1920s, he developed the trick process while shooting Fritz Lang’s “Metropolis”, which demanded giant sets. In order to keep production costs reasonable and to not lose too much time on building such a giant set, he created a set-up that, while using a partial mirror, only required a miniature model. (cf. Minden et al., 2002)

A mirror at an angle of 45 degrees is placed between camera and miniature set. At the parts of the image where live action is supposed to happen, the reflective surface of the mirror is removed so that the set located behind the partial mirror is visible (see Figure 29).

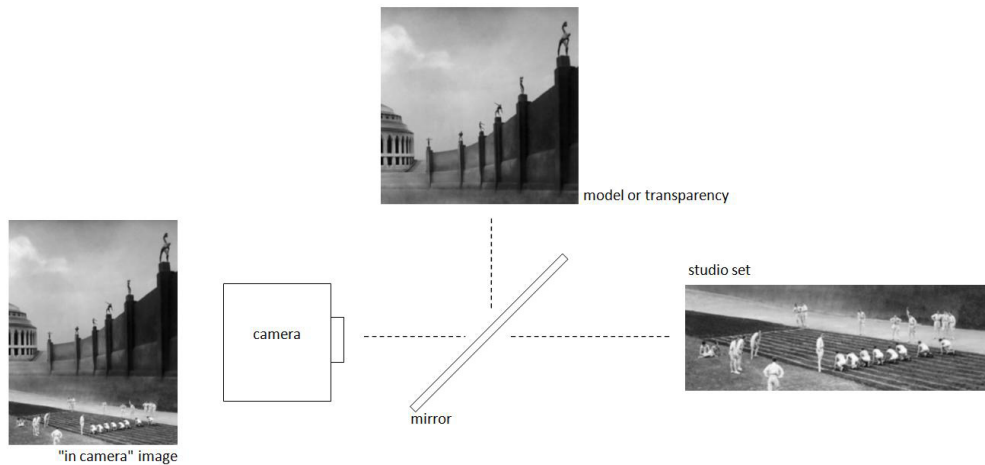


Figure 29: Schüfftan process applied in scene from Fritz Lang's "Metropolis".

Depending on the scene, parts of the image or a skeleton that match the rough architecture of the model have to be built to allow the reflected model and the live action to blend seamlessly.

In addition, special attention has to be paid to the lighting of the miniature model and the studio set to achieve a believable blend of the two parts. Further building miniature models or constructions same as lighting the scene and creating the mirror matte required highest precision. To illustrate the difficulties to create such shots, e.g. the road shot in Fritz Lang's "Metropolis" (Figure 30), it took 8 days of work and 40 meters (2100 frames) of film shooting model scenery as every frame had to be shot individually. The resulting shot was no longer than 10 seconds. (cf. *ibid.*) For these shots of the main road in Metropolis, all of the about 300 small model vehicles had to be moved a few millimetres forward after every single frame to create the impression of movement in the scene.



Figure 30: Producing the road scene in Metropolis via stop motion.

And this was not even the most difficult scene: For a scene where a machine hall should explode, the model construction and preparation took four weeks as it could only be shot once. (cf. *ibid.*)

Many other filmmakers like Alfred Hitchcock made use of the Schüfftan process in the first half of the 20th century. In Hitchcock's "Blackmail" the chase on the roof of the reading room of the British Museum was a miniature shot using the Schüfftan process, while only a skeleton ramp for the actors to run on was actually built. (cf. Cock, 2011)

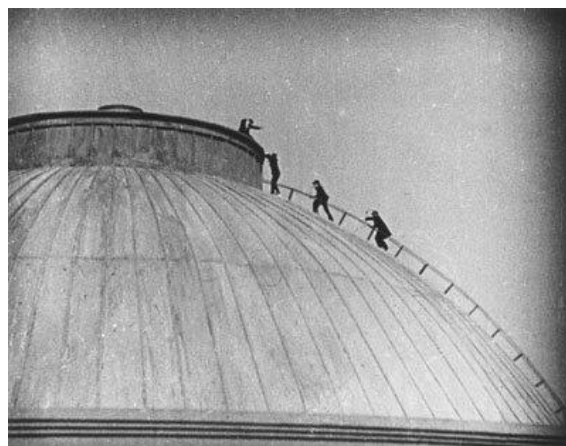


Figure 31: Actors seemingly on the roof of the British Museum in Hitchcock's "Blackmail".

Instead of the miniature model a photograph or drawing could also be shown on the reflective part of the mirror. It was also Hitchcock who used this method in "The 39 Steps" (1935). In the scene shown in Figure 32, only a few actors on the right side of the picture and the actor on the stage actually move. The whole other part of the scene is a

photograph or painting and the audience in fact does not move. However, as the scene is quite short, the attention is mainly given to the movement on the right side and the stage, so that the viewer fails to notice that the rest of the audience stays motionless.



Figure 32: Alfred Hitchcock using the Schüfftan Process in “The 39 Steps”.

Although this in-camera special effect is effective and also used to a great affect in films like “Metropolis”, the process was soon replaced by matte techniques offering more flexibility and the possibility of camera panning.

But Schüfftan's process was also used as recent as in Peter Jackson’s “The Lord of the Rings: Return of the King” in 2003 (Figure 33).



Figure 33: Applying the Schüfftan process in “Lord of the Rings”.

4.1.3 Other in-camera effects by means of reflections

A common method to capture high-angle shots, where the camera points down from above the action, is using a mirror. Instead of positioning the camera at a rig high above with the camera tilting down, which can be difficult because of safety reasons and camera operating problems, a mirror is placed at an angle so that the camera looking at the mirror sees the subject of the shot from above, as shown in Figure 34.

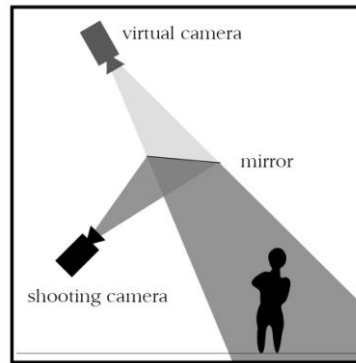


Figure 34: High-angle shot realized with a mirror.

The method with the mirror setup simplifies shooting extremely and, as the mirror itself is not in depth of focus (the focus distance is corresponding to the distance of the virtual camera and the subject), small dust particles usually are not visible in the captured images.

Another way to use a mirror to simplify a shooting setup was applied in the “space dive” scene in J. J. Abrams’ “Star Trek” in 2009. In the beginning, the actors were filmed on harnesses facing downwards with the camera facing upwards. Due to blood circulation issues and absence of the actors, they turned around the whole scene (Figure 35) with the camera pointing downward and the actors standing on mirrors so that the reflection of the sky shown in the mirror lets the actors appear falling from the sky. (cf. Bell, 2013) Finally with adding wind and camera motion, the sequence’s integrity of the originally planned shot was maintained due to the mirror setup.

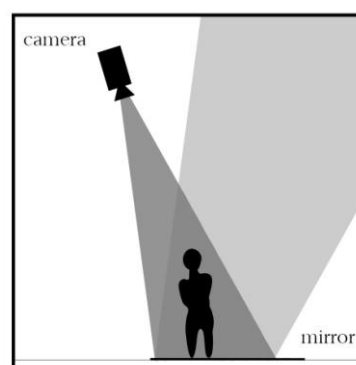


Figure 35: Realization of space jump scene in “Star Trek”, 2009.

Additionally, mirrors and reflectors are a common technique to enhance given lighting and to create flares. Placed at the right angle, reflectors and mirrors can quickly increase the light in parts of a scene. Further, white, silver or gold reflectors can add to the color temperature of a scene.

In particular, lens flares can literally be considered as in-camera effects which are caused by very bright sources of light – often not even located in the frame. Due to internal

reflection and refraction within the lens system, colorful artifacts usually appear with the shape of the iris of the lens. Most of the time, lens flares are not planned to occur but can add to an image's composition.

4.2 Reflections in today's visual effects

In the starting time of visual effects, reflections were vastly used to combine images in order to create in-camera effects, as described in the previous chapter. Today, reflections play a minor role in capturing moving images but a major role when working on the footage in postproduction.

4.2.1 Boon and bane of reflections

While scenes using reflective surfaces are usually hard to shoot, they will often need a hand of a visual effects artist to replace the reflective objects or make corrections, in order to achieve the scenes' meaning and to make it visually coherent.

Visual effects artists compose various layers together that are shot separately. Since the light characteristics are different in all layers, and light interaction is missing in total, compositors have to adjust the layers to make the image seamless. In “Snow White and the Huntsman” the visual integration of the CG “Mirror Man” was assured by using a mirrorlike representation of it on set, as shown in Figure 36 (left). The specular reflections of the actress on the counterpart could then be used as a reference in post-production to map the filmed reflection on the CG character, referring to Figure 36 (right).



Figure 36: Creating the “Mirror Man” by using a life-size reference.

However, if there are specular surfaces like mirrors, windows, cars, etc., a scene not intended as a visual effects shot becomes one because the reflection might reveal the camera and set unit if not shot in a suitable angle.

Even though placing highly reflective or semitransparent objects in a scene – which certainly could be avoided or solved with dull spray to diffuse the surface reflections – requires time and effort during both shooting and postproduction, the challenges certainly pay off in adding another dimension and brilliance to the scene. Specular reflections play an important role for the artistic concept and visual design of film and CGI, and add to a higher production value.



Figure 37: Reflections and refraction give rendered scenes a more realistic impression.

It has always been an allure for cinematographers to use reflective and refractive elements in a scene. The reason for this is on the one hand the fact that reflections always add another depth component, giving the viewer a more three-dimensional impression. On the other hand reflections open up another perspective that reveals the space from another angle than the camera sees it. It can give information about the scenery outside the frame helping the viewer to put an object into context without directly showing the surroundings.

Another key benefit of highly reflective surfaces is the fact that they add brilliance to an image as we associate shininess with valuable things like jewelry, cars, gold, etc. At the same time reflections offer important clues to the condition of a surface, as reflections divulge the presence of scratches, dirt or unevenness but also the smoothness, flawlessness and degree of perfection that the viewer subconsciously links to properties of the object itself. Car commercials are an evident example for the importance of a shiny, flawless, high reflective surface that gives an extravagant and brilliant impression of the product.

4.2.2 Replacement with 2D compositing solution

This chapter shows how to deal with different kinds of reflecting surfaces that are found in a film scene with simple 2D compositing.

The first case contemplated is a conventional shot containing unwanted objects in the reflection on a mirror, window, screen, i.e. rather plane specular (transparent) surfaces.

Already before shooting the scene some principle questions have to be considered:

What is visible in the reflection and what should be visible in the end?

An example would be that the reflection in a flat mirrorlike surface shows the actual or manipulated performance of the actor but also shows the camera or set unit. Then only a part of the reflection has to be retouched. Another case is that the whole set appears in the background and the acting contains a lot of movement, then the whole reflection would have to be exchanged.

Does the camera move?

If the camera is static, the replacement or retouch of the reflected image is fairly trivial and should not be problematic. With rotoscoping, painting and transforming, the desired result should be achieved. However, if the camera moves, there are some more steps to be proceeded.

First, camera movement needs to be evaluated. As the replaced reflection has to stick to the mirrorlike surface, match moving is required. Match moving describes “the process of matching CG elements into live-action footage.” (Dobbert, 2012, p. 1)

For a good match move a few tracking features are required. A feature is a specific spot in the frame that is recognizable for the tracking algorithm of a program⁸ and visible throughout a range of images. Suitable tracking features are usually high-contrast spots.

When the camera’s movement is simple panning, 1-2 tracking features are enough to compute a 2D track. If the camera moves in space and the corners of the reflective surface are visible throughout the sequence, a simple corner pin tracker or NukeX’s or Mocha’s planar tracker is able to replicate the image of the reflection. Planar tracking works by analyzing the relative movement of many points on a surface, and thus calculating the movement of the surface as a planar surface in 3D space. When there are not enough features to track or the surface itself is not static, the track can get unworkable.

⁸ Relating to visual effects software like The Foundry’s Nuke, Adobe AfterEffects or alike.

Whereas it needs 3D match moving, when the camera movement is more complex and the corners of the mirrorlike surface are not visible throughout the sequence. This process is described in detail in the 3D section 4.2.3.4.

Does the actor move in front of the reflective surface? If so, can the surface be replaced by blue, green or even black screen?

When the actor is moving in front of the reflective surface, there are different approaches to replace reflections of mirrors, windows, screens and other plane reflective surfaces.

To be able to extract the mirror surface in order to be able to replicate it digitally, it needs to be separated from the foreground. When having a lot of movement of the actor, it is best to place a keyable⁹ matte in its position. Here is an overview of the different approaches of green, black or marker screen.

- Green screen

Placing a solid green (or blue) chart instead of the reflective surface allows using a chroma key to separate a matte for foreground elements that occlude the green (or blue) surface. Since the green screen is a dull surface, it can be difficult to recover reflection information and behaviour to put back over the new reflection. Additionally, problems might be created from the green spilling over the foreground objects.

- Black screen

Especially for screen replacements or transparent surfaces like windows, having a black reflective surface results in an almost perfect representation of the reflections and smudges that might be on the screen or window. For screen replacement this is achieved by simply leaving the screen unilluminated, for replacing a windows background it is very helpful to place black molleton behind the transparent reflective glass pane. Since there is no light being emitted from the surface, putting the reflections back on top of the replaced image is simple. However, depending on the foreground objects occluding the surface, e.g. fingers interacting with the screen or hair dangling in front of the window, extracting a matte to separate the foreground from the reflective surface can be challenging and time consuming when using rotoscoping and luminance keying. Tracking can also be difficult. Placing some tracking markers on the screen or window might be needed but because there are dynamic reflections sliding over the surface, it can be difficult to remove them.

As the given reflections on black screen are a perfect representation, the result probably comes out best but this method can be quite difficult to handle.

⁹ Keyable means the possibility to extract the matte of the foreground.

- Marker Screen

Both of the previous approaches can make tracking quite difficult if there are not enough features surrounding the reflective surface. In fact, even if a small portion of reflections is sliding over the surface, tracking the surface can be impossible.

One approach to solve this problem is to fill the surface with tracking markers which enables planar tracking. However, it can be difficult to separate occluding foreground elements from the surface – especially with quickly moving foreground objects and therefore resulting motion blur.

In conclusion, there is no standard solution, like in most areas of visual effects. The best solution varies from shot to shot. Choosing a suitable approach by considering the advantages and disadvantages of each one can be valuable.

After extracting the matte for the foreground the reflection can be replaced, e.g. by the reverse shot that was shot additionally to eliminate undesired reflections.

In the movie “Divergent”, a mirror room scene was realized by capturing the actress on a green screen stage with different cameras. By duplicating and composing the plates with the various perspectives, the effect of a hall of mirrors is achieved.



Figure 38: Realizing the mirror room scene in “Divergent”.

The position of the “virtual” camera capturing the reverse image has to be located symmetrically to the initial camera position over the mirror axis (Figure 39) in consequence of the reflection law described in chapter 2.1.

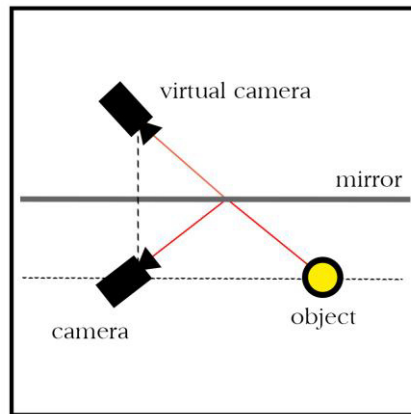


Figure 39: Virtual camera located behind the mirror to capture the reflection image.

Adding some streaks, dirt elements and light effects on the reflective surface, certainly always assists in convincingly integrating the inserted images as reflection.

In some cases, the described approaches can also be applied to non planar surfaces by warping and transforming the replaced reflection, e.g. reflection on iris of an eye. Whereas objects with a more complex shape or moving objects usually need to be replaced by 3D rendered elements.

4.2.3 Replacement with CG elements

Integrating computer generated imagery (CGI) and live-action footage to create a realistic scene with both blending seamlessly into each other is state of the art in the visual effects domain. To insert or replace specular CG objects convincingly, especially the shading and lighting but also texturing and rendering of a scene are of fundamental importance. To combine live-action footage and CG elements some principles have to be considered to achieve a visually consistent result.

4.2.3.1 Realistic reflection and shading models

Shading, which describes an object's surface response to light, is essential to adjust an object's appearance. Shading algorithms used in 3D applications are mostly based on the fundamentals of physics of real light. As described in chapter 2, there are several ways how light fractionally reflects off, passes through and is absorbed by a surface.

While a reflection or scattering model describes how light interacts with an object's surface at a point, a shading model describes how material characteristics vary across an object's surface. Together they are used to describe the appearance of a surface. (cf. Seymour, 2012)

To create a realistic result in computer graphics, the target is to compute the amount of light reflected from visible surfaces in a scene. A mathematical description of reflectance characteristics at a point of a non-transparent, opaque surface is the so-called bidirectional reflectance distribution function (BRDF) introduced by Nicodemus et al. (cf. Nicodemus et al., 1977) It describes the interaction of light with matter and is a 6D function. The BRDF is actually a simplification of the bidirectional subsurface scattering distribution function (BSSRDF) which is less standardized. In practice the BSSRDF is usually replaced by the component considering reflectance and transmission – the bidirectional reflectance distribution function (BRDF) and bidirectional transmittance distribution function (BTDF).

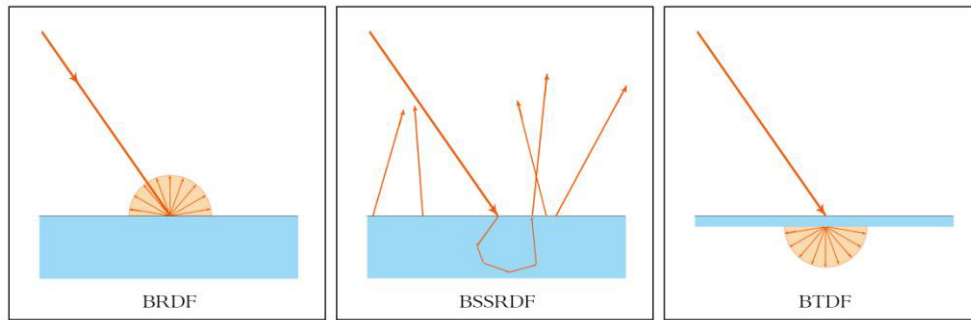


Figure 40: Visual simplification of the bidirectional functions.

The bidirectional reflectance distribution function depends on the following components: wavelength of the light λ , two spherical coordinates for the incident ray direction θ_i, ϕ_i and two for the reflected ray direction θ_r, ϕ_r plus the surface position u and v . (cf. Wynn, 2000, p. 3) It is bidirectional as it depends on two directions and the surface position. Thus, the BRDF can be described as $BRDF_\lambda(\theta_i, \phi_i, \theta_r, \phi_r, u, v)$. Referring to Figure 41, the “BRDF is defined as the ratio of quantity of reflected light [L_r at a position \vec{x}] in the direction $\vec{\omega}_r$, to the amount of incoming light [L_i reaching a position \vec{x}] from direction $\vec{\omega}_i$.” (ibid., p. 7)

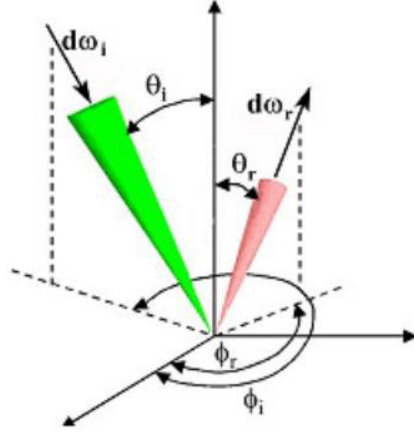


Figure 41: The BRDF's parameters with radiance of the incident beam L_i (green) and the radiance of the reflected beam L_r (red).

Each direction $\vec{\omega}$ is parameterized by θ and ϕ . Thereby, $d\omega$ is a solid angle element. \vec{x} is the position vector of the surface point. The amount of incident light reaching from direction $\vec{\omega}_i$ is E_i . Therefore, the BRDF results as follows:

$$\text{BRDF} = \frac{L_r}{E_i}$$

$$\text{with } E_i = L_i \cos \theta_i d\vec{\omega}_i. \text{ (cf. ibid., p. 7f)}$$

And therefore, the BRDF is given by:

$$\text{BRDF}(\vec{\omega}_r, \vec{x}, \vec{\omega}_i) = \frac{L_r(\vec{\omega}_r, \vec{x})}{L_i(\vec{\omega}_i, \vec{x}) \cos \theta_i d\vec{\omega}_i}$$

The BRDF has units of inverse steradians (sr^{-1}) with steradians being solid angle units. (cf. ibid., p. 8)

BRDFs are considered to be physically plausible, if they obey the conservation of energy and the reciprocity property. The reciprocity basically states that the BRDF stays unchanged if incident and outgoing directions are interchanged. (cf. Ahmed, 2004, p. 25)

Mathematically, this can be written as $\text{BRDF}_\lambda(\theta_i, \phi_i, \theta_o, \phi_o) = \text{BRDF}_\lambda(\theta_o, \phi_o, \theta_i, \phi_i)$.

The conservation of energy states that when light from a single incident direction interacts with matter and is reflected over a range of outgoing directions, the total quantity of light that is reflected and absorbed cannot exceed the original quantity of incoming light (Figure 42). (cf. Wynn, 2000, p. 9)

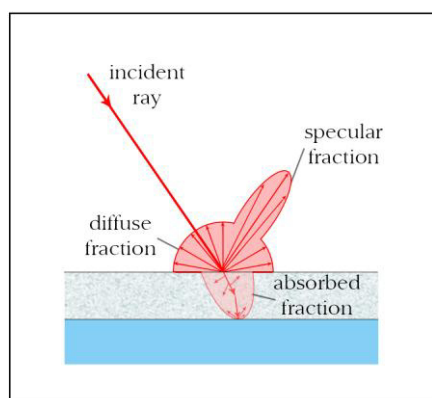


Figure 42: Conservation of Energy. The quantity of reflected and absorbed light must be equal to the quantity of incoming light.

As our perception of materials is largely determined by its reflectance characteristics, several different BRDF models have been established, which differ in effectiveness, efficiency and outcome, such as Lambert, Phong, Phong-Blinn and others. Two of the earliest shading models are Lambert shading and Phong shading. While the Lambert model results in smooth diffuse surfaces, Phong shading additionally models shiny highlights.

Besides the shading, the lighting has a great impact on the appearance of a surface. When adjusting the lighting to real-world footage, a reference image of a grey ball placed at the corresponding position on set, ideally taken with the shooting camera, can assist in achieving a realistic result.

There are different types of light sources in CG¹⁰: point light, spotlight, directional light and area light. While point lights and spotlights send out rays from an infinitely small point in space, directional lights illuminate the whole scene in a determined direction and not from a specific point. Further, area lights refer to a light emitting surface – with the intensity and shadow softness depending on the size of the area light.

Most common types of light in a CG scene send out rays from a small point in space – except for area lights radiating from a scalable area. However, as highlights are a reflection of the light source, point lights would produce only a tiny specular highlight – even too small to see. Thus, in order to solve this problem, shading algorithms in 3D software allow control over highlight size to enlarge the highlights. To achieve realistic shading it is important to give the specular highlights an appropriate size but also color, shape and position. As there are plenty of surfaces in real-world environment, it is best to adjust the

¹⁰ computer graphics

specular highlight based on a real-world example of the material rather than relying on presets given in the CG software.

The size of the highlights depends on the one hand on material properties, on the other hand on the size and distance of the light source. The highlight on the surface should be small, if the light source is small or far away. If the light source is close or large, a large highlight is expected.

Highlights may also be layered over each other to simulate real surface, e.g. coated with shellac, wax, liquids, etc. to add realism to the rendering. Multiple highlights can lead to a more adequate result when layering tighter highlights on top of broad and soft highlights. (cf. Birn, 2000, p. 251)

Anisotropic highlights that are stretched in a direction that changes, depending on the surface orientation, as described in chapter 0, require a specific anisotropic BSDF which can be found in almost all 3D applications. With attributes of anisotropic materials the orientation and rotation can be determined and also the spread of grooves, roughness and reflectivity.



Figure 43: Changing appearance with different anisotropy values. Left: anisotropy = 1.0, center: anisotropy = 4.0, right: anisotropy = 8.0.

As described in chapter 2.1.3 and illustrated in Figure 44, the reflectance and transmittance of a surface depends on the viewing angle referring to the Fresnel equations. A shader that implements these principles is often called Fresnel shader.



Figure 44: The reflectance of the specular floor varies with the viewing angle.

Often a control for the amount of the Fresnel effect is given with Fresnel scale, index of refraction, etc. Other parameters such as transparency and color allow fine tuning.



Figure 45: High ratio of transmittance (left), high ratio of reflectance (right), according to Fresnel equations.

A way to influence the amount of reflectance across a surface is specular mapping. Specular maps usually include the whole range of values from black to white. While white tones will bring up the full reflectivity of the highlights, black tones will block them completely. (cf. Okun et al., 2010, p. 615) Specular maps do not create specularities, but will determine the intensity of given ones. These maps can also consist of color values which will tint the reflections correspondingly. An applied specular map, e.g. on a human face model, can determine the areas where the skin is shiny and where it is more diffuse, as shown in Figure 46.



Figure 46: Specular map of a face.

As described in this chapter, considering the reflections, there are various aspects that add to the realism of a properly shaded object. In which way a surface responds to light is very important to achieve seamless and realistic results in order to then integrate into a real-world scene.

4.2.3.2 Image-based lighting

An important part of realistic rendering is image-based lighting (IBL). It refers to the process of illuminating a scene with light that is emitted based on an image from a real environment – the so called light probe image. It contains capturing an omni-directional representation of light information of the corresponding set or real-world lighting as a high dynamic range image (HDRI).

It can be created in one of three ways:

- Stitching together a mosaic of a series of stills created from multiple exposures of the same shot, i.e. High Dynamic Range (HDR) images which are often taken with a very wide or fisheye lens. Therefore, the photo camera is in the best case set up where the CG object will be located in the shot. Using a panorama head a series of bracketed stills by rotating the camera around its optical centre are taken.

Once the normal baseline exposure is determined, the exposures above and below will be bracketed, as illustrated in Figure 47. If capturing JPEGs, 1 f-stop or exposure value (EV) increment is required, i.e. images with EV -3, -2, -1, N, +1, +2, +3. If shooting in RAW, capturing images in 2 (EV) increment is sufficient, i.e. -2, N, +2. The number of brackets has moreover to be adjusted to the given contrast of the scene.



Figure 47: Exposure bracketing and final HDR.

It is advisable to use a cable release or the self-timing function to eliminate camera movement.

The rotation angle between overlapping tiles has to be adjusted to the lens and resolution. The set of images should be overlapping about 30 % to create a 360-degree panorama. (cf. Aithadi et al., 2006, p. 56) Additionally to the horizontal strip

of the panorama, two more strips with the camera pointing downwards and upwards should be made.

When the bracketed images are stitched together, the resulting HDR image has a wider dynamic range than the single exposures that represent only a small fraction of the dynamic range – the ratio between brightest and dimmest region. This means that when an area of a scene is extremely bright, the corresponding “pixels saturate to their maximum value no matter how bright they really are.” (Debevec, 2002, p. 27) In HDR images the pixel values are truly proportional to quantities of light. The combined images with multiple exposure bracketing can accommodate the huge range that natural lighting can have. (cf. *ibid.*)

However, if there are images of pure black (underexposed) or pure white (overexposed), they should not be used when generating the HDR file as they adulterate the result.

Creating the HDR files from the multi exposure images can be accomplished in Photoshop, HDRshop, etc. It is important to save them in a format that supports floating point values like OpenEXR(.exr), the 32-bit floating point version of TIFF (.tif) and radiance (.hdr) – and not as JPEG, 8-bit TIFF (only RGB color space) or RAW. Otherwise most of the generated data will be lost.

The stitching of the HDR images in order to create the final light probe image can also be done in applications like PTGui, HDRshop, etc.



Figure 48: High dynamic range image.

- Bracketed photographing of a chrome ball is an alternative to shooting a HDR panorama of the set. The chrome ball (or mirror ball), also provides the necessary data needed to set up IBL. For complete coverage of the set, the chrome ball needs to be photographed twice from opposite sides, since the back of the ball (in Figure 49 referred to as blind spot) is not covered in the reflection.

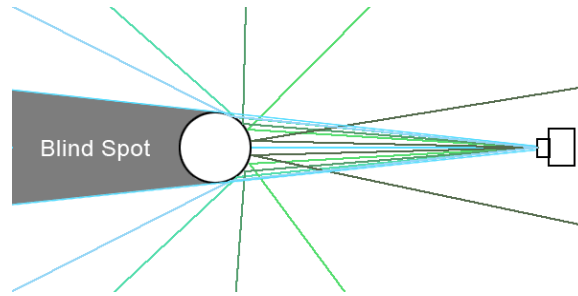


Figure 49: Chrome ball captures do not cover a 360 degree panorama.

However, if there is only time to capture one angle of the chrome ball, applications can fill in the blind spot. Then, the images should be taken from the direction the film camera will be shooting. The mirror ball should approximately be placed at the location where the CG element will be inserted. Camera set-up and location should be adjusted so that the chrome ball fills the frame but is not cropped to get a good resolution of the reflection. Further, it should be achieved to have a small reflection of the camera and the photographer himself, as this will otherwise affect the final lighting.

If possible, the chrome ball images should be taken from a distant position with a long focal length (Figure 50) at the same level as the chrome ball.

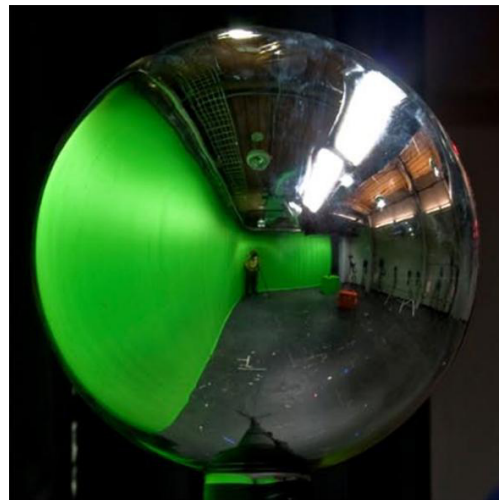


Figure 50: A small reflection of the camera itself will be easy to remove.

Another advantage of the distant location of the camera is that the blind spot opposite of the camera is then minimized, as illustrated in Figure 49.

Stitching together the captured multi exposure images works as described above for the HDR panorama.

The chrome ball method is less effort and less time consuming as the HDR panorama, thanks to reflectance characteristics. However, the quality is worse because of the compression on the sides of the mirror ball (referring to chapter 3.1.4).

- A final method to create a light probe image is using a special panoramic camera, such as Panoscan, Sphereon, etc., which contains several image sensors on a rotating camera head allowing captures of a 360° HDR images. (cf. Debevec, 2002, p. 27)

Further, these light probe images can be projected onto a sphere or dome analogously to environment mapping¹¹ in 3D applications like Maya, Blender, 3ds Max, etc. (cf. Seymour, 2012) It is an indirect illumination method based on a HDR light probe considering the bright areas as lights. Thus, the scene will be illuminated corresponding to the properties of the HDR image and further reflections from this light probe image will also appear on the models' surfaces, as demonstrated in Figure 51.



Figure 51: Image-based lighting with a light probe image mapped on a sphere.

In summary, image-based lighting is used to simulate the lighting for the objects in the scene, allowing highly detailed real-world illumination and thus also reflections of the real world based on the light probe image. Therefore, IBL is an effective and accurate tool for lighting and rendering a scene to integrate CG elements into live action footage.

4.2.3.3 Ray-tracing

Ray-tracing is another approach to modeling the properties of reflectance. Ray-tracing describes a technique for rendering a photo-realistic image by tracing light paths. In real environment, most light sources emit streams of photons in all directions which are then reflected several times of various objects. An object is seen by a person when some of these photons are on a path that enters the eyes, stimulating the receptors on the retina at

¹¹ Environment or reflection mapping is a method of rendering a reflective surface by means of a mapped texture.

the back of the eyeball. Simulating this procedure in computer graphics would not be efficient as there are too many photons to trace and only a small fraction of photons appear on the image in the end. Optimizing this procedure, ray-tracing algorithms send out light rays backwards – from the camera into the scene (Figure 52). (cf. Ross, 2014, p. 6)

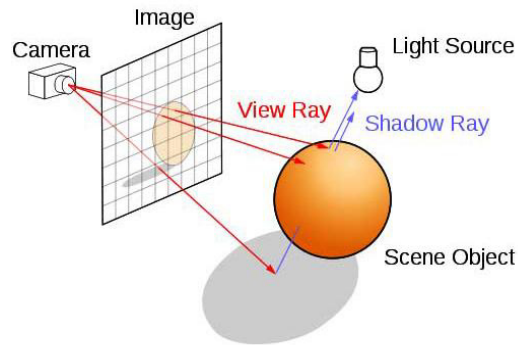


Figure 52: Basic ray-tracing method.

Each pixel on the image plane is assigned to a color value depending on the information computed on a ray's trace.

Launching from the camera, a primary ray is sent out for every pixel of the image plane. For every primary ray, the intersection with the nearest object is calculated. Further, the color of the intersection point is computed depending on the surface shading, the reflectance characteristics, the light color and the light intensity.

As shown in Figure 53, so-called shadow rays might also be shot towards each light source, to check whether the intersection point on an object is lit or covered from each light source by an interjacent object. If there are intersections tracing the shadow ray towards a light source, the point is hidden from the light source. If there is no intersection on the shadow ray trace, the point is lit by the light source. Light shaders then contribute to the calculated amount of illumination.

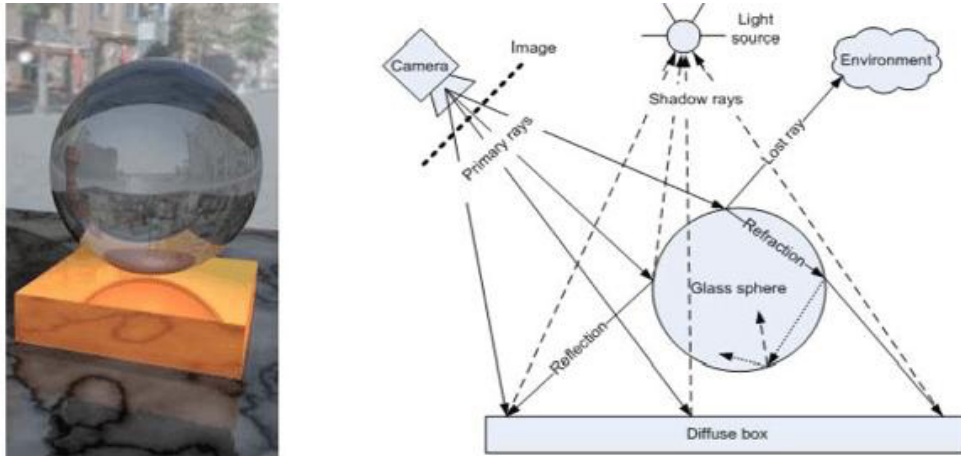


Figure 53: Ray-tracing modeling and light paths.

To involve reflections from other surfaces and also refraction through the surface, secondary rays are exhibited to simulate the ray path affected by the reflectance properties of the object's surface shader. Secondary rays can, in turn, hit other surface shaders and thus activate additional rays, which are then reflected in recursive procedure, until they do not further significantly contribute to the image. Ray-tracing recursion is stopped by a determined depth limit, i.e. a threshold for the amount of ray iterations (Figure 54).

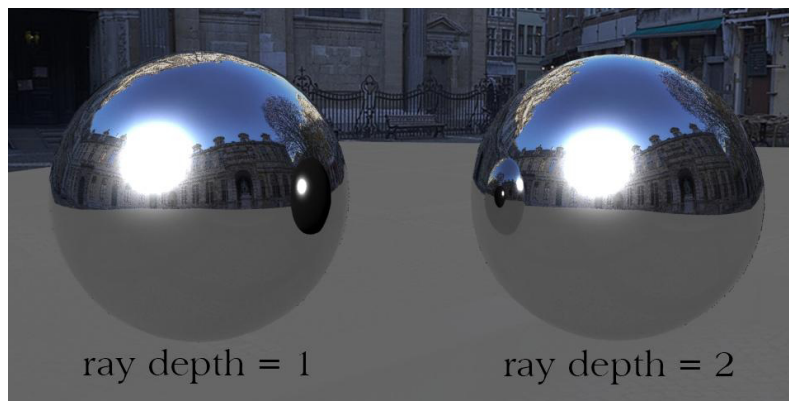


Figure 54: The number of reflections increases with ray depth.

If a ray did not hit any object or light source, a so-called “lost” ray, usually an environment shader is applied. So once a ray hits a surface, the shading model is computed and determines the further process, otherwise the program calculates an infinite number of light rays.

Ray-tracing occurs on a pixel-by-pixel basis, until the whole plane of pixels is colored. Further the amount of pixels depends on the resolution. The goal of the ray-tracing algorithm is to find and evaluate the sent out ray's intersections with objects in the scene. Then, it determines the surface normal at the intersection in order to find out the reverse direction of the ray sent out from the camera position. Ray-tracing is based on the physics of light enabling accurate reflection, refraction and shadows. However, the result of a

standard ray-traced reflection on a surface might appear too perfect, as surfaces in reality blur and distort the reflections due to material properties. Some ray-tracing algorithms allow soft reflection that scatters or randomizes ray reflection in order to create a natural, more blurred reflection. It combines the crisp reflection of nearby objects with a more diffuse light reflection. While a standard ray-tracer pictures purely specular reflections, a soft ray-traced reflection is glossier. Even though soft ray-tracing increases rendering time, it adds to the realism of the rendering. (cf. Birn, 2000, p. 235–236)

Direct lighting is usually best succeeded using backwards ray tracing. However, specific indirect effects, such as caustic, usually profit from rays generated from the light source instead of the camera. Caustic describes the light pattern which is formed by bundled light rays being reflected or refracted of a curved object onto another surface, as shown in Figure 55 (right). In nature, caustic patterns can easily be observed, e.g. on the ground of a swimming pool, in the inside of a coffee mug (Figure 55) or when a ring lays on a surface.

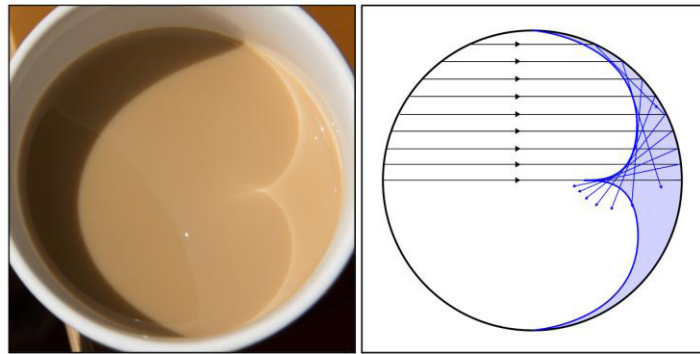


Figure 55: Caustic arising from sun light reflecting off a mug's curved inside.

In rendered scenes, caustic effects can contribute to a more realistic and natural result. An algorithm that traces light rays from the light source onto reflective objects, following their paths to the camera, will better sample this caustic light effect as backwards ray-tracing from the camera.

The implementation of both the camera and light source sending out rays, is designated as bidirectional path tracing. The differently constructed path rays are connected to each other after a distinct amount of bounces.

There are several other methods including more sophisticated techniques than the basic ray-tracing algorithm. Another method, which also quickly samples caustic, is photon mapping. The realism of this ray tracing method is increased by simulating photons being emitted from a light source and from the camera and then bouncing around the scene.

To sum up, there are various different ray-tracing algorithms that vary on the one hand in efficiency, i.e. rendering time, realistic performance and quality and on the other hand in their capability to render indirect light, reflections, refractions and features like caustics.

4.2.3.4 Match moving

In order to seamlessly integrate CG elements into a filmed plate, the real three-dimensional camera's motion has to be transferred on the CG element. This procedure is referred to as match moving, which can be accomplished in various match move applications such as SynthEyes, Boujou, PFTrack, etc. and in 3D match moving tools for compositing applications, such as the Camera Tracker in NukeX or Mocca for After Effects.

For a good 3D match move it is essential to have enough stable features in the scene; there continuously have to be at least 7 features in order to get a proper camera solve. If there are not enough features in the filmed plate, it will be difficult to compute an applicable camera track. Therefore, tracking points might be placed into the scene before shooting, diligently estimating their use and effort to replace them afterwards again.

Once a solid 3D camera track is accomplished, the camera including its movement can be imported into the 3D application used to generate the reflective object.

Here it is important not to do it vice versa, i.e. importing the rendered CG element first to insert it into the compositing tool to then apply it on the camera track. The object would move along with the camera movement; the reflection, however, would deadly stick to the surface, as reflections are viewer dependant.

If modeled in real world scale, the camera can be placed in the 3D space in relation to the generated scene. Tracking markers can also be imported into 3D space of the generated scene, giving information about the tracked features' location in space. Thus, it makes sense to track a feature on the same approximate location and depth plane as the generated object will be placed. The further away from the corresponding depth level the CG object is located, the more it will drift and slide when compositing, i.e. it requires additional adjustments later.

If not modeled in real world scale, the track can simply be adjusted by scaling and repositioning the track's motion.

So far, the case of a moving camera was contemplated. In cases where the camera and the reflective object are both moving, match moving becomes more complicated. The

solver can then no longer evaluate the movement between static features relative to the camera, as the feature's motion could derive from the camera's movement and the movement of the object. (cf. Dobbert, 2012, p. 238) Even though some match moving applications are capable to distinguish between camera and object motion, achieving a good result can still be difficult.

Tracking an object's motion with static camera works in a similar way to tracking camera motion with static environment. Here, after tracking the scene's camera motion (that is actually static), this motion can be inverted onto the object. (cf. *ibid.*, p. 227)

Object tracking can sometimes have problems with the nature of the object's motion itself. For instance, when the object rotates back and forth, some of the features will be occluded by the object itself. (cf. *ibid.*, p. 277) Another problem can be caused by reflections when tracking a reflective object's motion, as they might modify tracking features and make them unrecognizable for the solver. Although this might not make the tracking impossible, it certainly makes it more difficult and tedious. Once more, this is evidence that it is essential to think about match moving before capturing a scene and how to avoid problems, e.g. by using a dull object instead of a reflective one.

Another essential issue is gathering information while on set. References about set dimensions, prop measurements and especially camera setups, like focal length, are very important to achieve an accurate match move.

A general consideration to lens distortion has to be made when merging live-action footage with CGI. Lens distortion generally derives from optical aberration that bends and deforms physically straight lines to curvy lines in the captured image. It actually is a lens error that does not exist in CGI. Even if the CG element is rather small, applying lens distortion helps to naturally fit it into the live-action plate. However, distorting a plate always results in a loss of data and resolution. Therefore it is recommended to render an overscan in order to have an additional area at each side to apply the distortion.

Concerning lens distortion, the workflow will usually be as follows:

First, the live-action footage needs to be undistorted, i.e. correct the lens distortion. Then the undistorted scene is match moved and solved for a camera motion, which is imported into the CG scene. Overscanning by a certain percentage or rendering out the CG plate at a slightly larger resolution then follows. Finally, after rendering the CG scene including the camera motion, distortion is applied onto the CG plate; it is reformatted to the original resolution and then merged together with the untouched real-action footage.

4.2.3.5 Rendering passes and compositing

Compositing computer generated elements with live-action footage highly profits from rendering passes of the CG objects. Rendering in passes describes the process of rendering different attributes of the scene separately. The resulting multi-pass images, i.e. images with various passes each with different attributes, allow high degree of flexibility and control over the final look of the shot.

The most commonly used passes are the beauty pass, diffuse pass, specular pass, reflection pass, shadow pass, depth pass, ambient occlusion pass, motion vector, etc., as shown in Figure 56. (cf. Zhi, 2013, p. 250)



Figure 56: Combining different render passes to a final composite.

The separate render passes can be combined together to achieve a satisfying result by using mathematic formulas in a compositing software like Nuke. Rendering passes are a huge advantage for compositors as they can e.g. adjust the lighting of a scene, intensify an object's reflections, add motion blur, etc. without affecting other layers and without having to re-render in 3D software. By adjusting the different passes individually a scene can be improved interactively. Additionally, the scene's rendered passes can be precisely fine-tuned and matched to the live-action plate. (cf. *ibid.*)

For creating realistic reflections on a CG element, the diffuse pass, specular pass, reflection pass, refraction pass are the most important rendering passes.

The diffuse pass, is the rendering containing most of the color values and detail of the element that includes diffuse illumination but neither reflections, speculars nor shadows. It usually comes with an alpha channel useful for compositing the object over the background plate.

Specular or highlight passes isolate specular highlights from the object. Any other types of shading are eliminated. A separate specular pass allows more possibilities to render the specular reflections. As an example, a bump map could be applied to give some variation to the highlights, although it was not applied on the diffuse pass. Or the light source could be moved slightly in order to achieve a more pleasing result. However, not all shaders have specular capability such as the Lambert shader.

In compositing a specular pass can be composited over the diffuse pass with an *Add* or *Screen* operation. Applying these merge operations, brighter areas of the specular pass brighten the diffuse pass, black and darker areas of the specular pass then have no effect on the diffuse pass and no alpha channel is required. (cf. Birn, 2000, p. 258)

Furthermore, a separate specular pass allows adjusting the brightness and color in order to match to the rest of the scene. Adding a glow effect during compositing is owing to the separate specular pass very easy. It only needs a blurred copy of the specular pass to create a glow around the highlights.

In contrast to the specular pass that contains reflections of the light source, the reflection pass shows the reflections of other objects or the surrounding scene.

Reflections and refractions are treated very similarly in rendering and thus in compositing same techniques can be used. Reflection and refraction passes are composited into a scene through *Add* operation. (cf. Novosad, 2010, p. 44)

Compositing the diffuse pass, specular pass and reflection pass together an *Add* or *Screen* operation can be applied. The *Add* operation adds values of the two images as $a + b$, whereas the *Screen* operation calculates $1 - (1 - a) * (1 - b)$. Often the *Add* operation is applied as it creates a more realistic result. However with the *Screen* operation it is less likely to have clipping problems in bright areas as pure white is rarely reached. Concerning specular highlights this can be important.

Sometimes the generated object also casts a reflection onto a surface in the live action footage, e.g. a water surface, a shiny floor, a glass bottle etc. To have a maximum of flexibility this cast reflection should be rendered as a separate reflection pass. If the surface receiving the reflection is given in the live-action plate, it needs to be modeled and positioned in 3D space according to the given scene in the footage. When the object moves in the filmed footage, it also needs to be animated in a way that the reflections move along. Considering a water surface, a bump map can help simulating water ripples.

If the object receiving reflections is another computer generated 3D object, the object itself has to be made visible and reflective to render the separate pass. (cf. Birn, 2000, p. 261)

Rendered reflections often suffer from having too much color and contrast which can fail to look realistic. To match the reflections to the background plate usually color and contrast adjustments need to be applied.

This chapter gave an insight into the components of digital compositing and CGI operations with the aim to realistically integrate rendered specular objects into live-action plates. There are several factors contributing to a harmonious visual final composite such as the choice of reflection and shading models, the decision on lighting and rendering methods for the CG scene. However, reflections also require a very good match move and an eye for adapting render passes to complete the integration.

5 Transferring reflections from the real world to digital 3/2,5D space

5.1 Stereoscopy with reflective and glossy surfaces

5.1.1 Stereoscopy fundamentals

Stereoscopy describes a technique that allows three-dimensional perception by creating the illusion of depth by means of 2D images. Stereoscopic movie making is closely related to binocular vision considering the joining of two images – each with a slightly different perspective – of a three-dimensional visual scene. Even though the term stereo 3D is well-established for stereoscopic movies, viewing two flat images clearly differs from viewing three full dimensions. This means that, in contrast to real three-dimensional space, the viewer cannot receive more information about three-dimensional space by head or eye movement. A more appropriate term for this certainly would be 2,5D.

Nevertheless, stereoscopy tries to imitate binocular vision to add depth to captured images of a scene by using 2 cameras at a slightly different position correspondingly to the eyes' location on a human's face; this horizontal offset creates binocular disparity.

While presenting the right images to the right eye and the left images to the left eye, the visual system fuses these two images and sets up a pretended three-dimensional space, i.e. the perception of depth is accomplished.

The cameras' positions to each other have an impact on the perceived depth. The distance between the two centers of the camera lenses when aligned parallel is referred to as interaxial distance. (cf. Dashwood, 2011)

The wider the interaxial distance, the more depth is created as demonstrated in Figure 57.

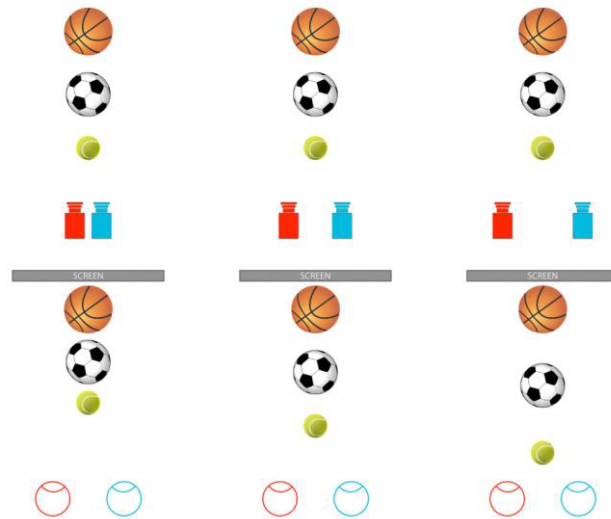


Figure 57: The impact of interaxial distance on the perception of depth.

The two cameras can also be placed angled towards each other, corresponding to the angle formed by the eyes in order to target an object, which is referred to as convergence. The eyes' fixation point can consequentially be considered as the convergence point for the two cameras. The convergence point appears at the screen plane for the viewer. Objects closer to the convergence point appear in front of the screen, whereas objects behind the convergence point appear behind the screen (Figure 58).

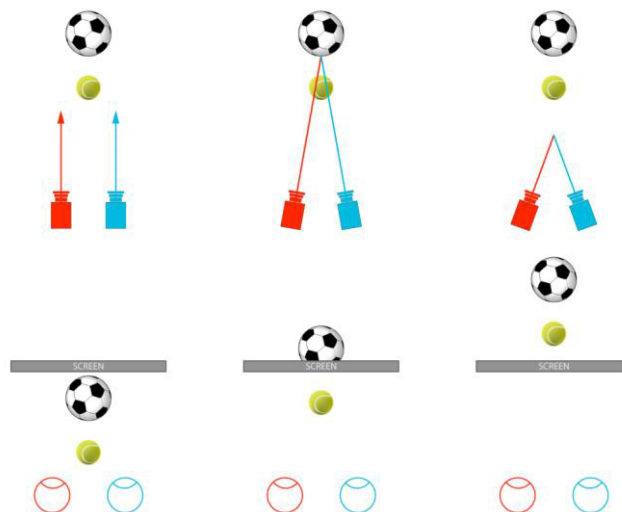


Figure 58: An object's position in relation to the screen is determined by the convergence point.

In case of two parallel cameras (Figure 58, on the left), i.e. they aim straight ahead, there is no convergence which induces that the point of convergence is set to infinity. Accordingly, infinity is placed on the screen plane and all elements appear in front of it. This allows adjusting the convergence point in postproduction. By shifting the two images horizontally, the convergence point can be placed wherever desired. (cf. Wright, 2011)

In case of converged cameras, the convergence point is already “baked in”. However, this can also be adjusted in post production by shifting the two views horizontally, but can cause problems due to the distortion of each camera. (cf. *ibid.*)

According to binocular disparity and crossed and uncrossed diplopia (cf. chapter 3.2.1), objects in front or behind the convergence point appear separated on the display screen. This separation is here referred to as parallax. Objects appearing at the screen plane have zero parallax which means that the object in the left and right image is in the same position. (cf. Reeve et al., 2010, p. 7) Objects appearing behind the screen have positive parallax as the image is shifted to the left for the left eye and to the right for the right eye, whereas objects appearing in front of the screen have negative parallax as the image is shifted to the right for the left eye and to the left for the right eye. (cf. *ibid.*)

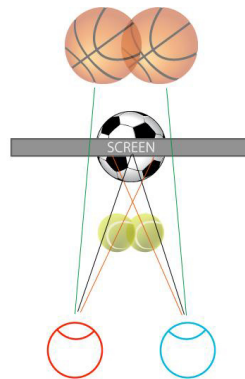


Figure 59: Positive parallax for more distant objects (green line), negative parallax for closer objects (orange line).

As viewing big differences and fast changes between positive and negative parallax can cause visual discomfort, it is important to consider the limit of usable depth. The so called depth budget represents “a percentage between the left and right eyes’ separation in relation to screen width.” (Reeve et al., 2010, p. 9). Therefore, it is depending on the screen size and the viewers distance to it. A critical limit of depth budget would be approximately 3 % of the horizontal resolution of an image. (cf. Knorr, 2011, p. 13) Without getting deeper into this matter, it can be stated: Too much depth in a shot deriving from too much interaxial separation can cause stress to the audience not being able to fuse the images. That means larger interaxial distance can be used for more distant scenery without closer elements. Smaller interaxial distance is suitable for close-ups without very distant objects.

All this needs to be considered, when setting up a stereo shoot which will be described in the next chapter.

5.1.2 Capturing stereo 3D

There are several different approaches to capture stereoscopic images to simulate stereoscopic vision. The two most common ones are with a side-by-side rig and with a mirror rig.

A simple way to capture stereo 3D, is having a side-by-side rig, i.e. cameras are mounted side-by-side. Usually horizontally, they are aligned parallel or angulated to each other.

Shooting stereo 3D, the interaxial distance is an important parameter which is responsible for the depth effect. The width of two cameras bodies and the size of the lenses limit the minimum interaxial separation in a side-by-side rig. (cf. Dashwood, 2011) As mentioned in the previous chapter, this interaxial distance is suitable for shots like overviews, landscape, wide angle, helicopter shots, etc. but too wide for the close-ups and also usual live-action scenes.



Figure 60: Left: side-by-side rig, right: beam-splitter rig.

The latter can better be captured by a mirror rig. There are several possible arrangements to align two cameras to direct images via a mirror (Figure 61).

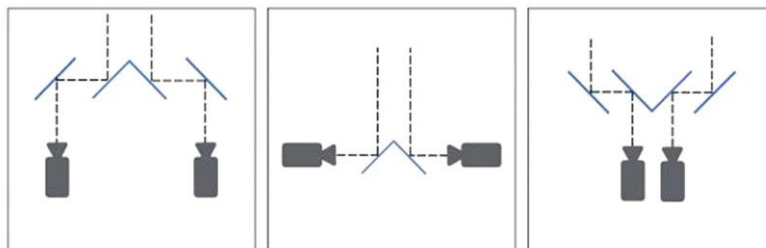


Figure 61: Different constructions to direct the two images with mirrors.

However, the most established approach is with a beam-splitter rig where two cameras are aligned in a 90° angle both facing the beam-splitter (Figure 62). One camera looks right through the beam-splitter, the other one can be placed above, below or even at the side looking at the reflection on the mirror. Due to imbalance reasons, the adjustment of

the camera at the side is used very rarely. Additionally, the mirror would have to be much bigger in size. For static shots, the most common arrangement is the one with the first camera directly facing the scene and the second camera above pointing downwards on the beam-splitter. In that way, the first camera can easily be mounted on a tripod and panning is trouble-free.

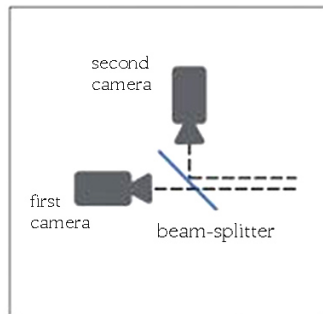


Figure 62: Standard beam-splitter rig.

As described in chapter 4.1.1, on a beam-splitter or two-way mirror 50 % of the incident light is transmitted and 50 % reflected at a time.

A big advantage of a beam-splitter rig is that the interaxial distance can be decreased to 0 mm (= 2D) which allows using the camera images for geometrical alignment of the cameras. (cf. *ibid.*) Due to the possibility of small interaxial distance, beam-splitter rigs are good for shooting classical movie scenes like close-up, detail and dialogue shots.

But the beam-splitter rig has also some disadvantages. The beam-splitter itself is responsible for loss of light as the light is split up for the two images. In addition, the rig's size, its bulkiness and the susceptibility to damage are disadvantageous. Further, the beam-splitter is one more optical element that has to be handled and produced with care which usually leads to a higher price than the side-by-side rig. Other concerns are dust, scratches or fingerprints on the surface of the beam-splitter. (cf. Tauer, 2010, p. 391f) Moreover, mirrors filter light according to its polarization which results in brightness and color differences between the two images – particularly concerning reflective and transparent elements. As the beam-splitter creates different light polarization for the two cameras, specular reflections and specularities are often distorted.

There are some more ways to capture stereoscopic 3D, e.g. with stereoscopic lenses or stereoscopic camera, but using the side-by-side and beam-splitter rig are the most established ones.

5.1.3 Problems and irritations related to reflections

In stereoscopic images, problems with reflections can cause irritations. These problems can be eliminated on set, if recognized during shooting. If these problems only become obvious after the shoot, it usually requires challenging postproduction processes to solve them.

5.1.3.1 Beam-splitter reflection

One component responsible for not matching reflections is the beam-splitter polarization. Reflective surfaces polarize light in a direction depending on the material's atomic structure and incidence angle of the light. Light reflected from a glossy surface, thus polarized light, reaches the beam-splitter; the polarized light is unaffectedly transmitted to one camera, whereas it is filtered out from the reflecting light path reaching the other camera. As a result, the camera looking through the beam-splitter receives more light than the camera looking at the reflection. Additionally, the reflectance of the reflected image is not spatially equal but depends on the angle of incidence, referring to Figure 5. There are two ways to solve this problem with polarization filters.

One is to insert a linear polarization filter in front of the camera looking through the beam-splitter in order to simulate the light-filtering that occurs when light is reflected on the beam-splitter. (cf. Mendiburu et al., 2011, p. 41) Hence, the two cameras receive the same polarized light. However, this polarization filter leads to a reduction of light and so the other camera is required to even out the different light level. (cf. *ibid.*) This is usually related to one exposure stop reduction. Hence, this solution with a polarization filter consumes one more exposure stop on both cameras. As the two-way mirror already causes a loss of one exposure stop, this leads to two exposure stops reduction in total.

Another solution without that much loss of light is to use a circular polarizing filter that creates circularly polarized light. (cf. *ibid.*) By placing the circularizing filter in front of the beam-splitter, all light waves are circularly polarized and are less affected by the beam-splitter. (cf. *ibid.*)

One more problem with the beam-splitter method is the fact that, depending on the rig, the reflected image is usually upside down, i.e. flipped vertically and horizontally. (cf. Stump, 2014) Cameras with rolling shutter scan the scene line by line, from top to bottom and from left to right. In case of the upside down image, the camera seeing the reflected

image on the beam-splitter, scans it from bottom to top. Especially for dynamic scenes, i.e. fast moving objects or camera motion, objects in the scene seem to be skewed as the camera minimally lags behind with scanning motion. Due to upside down images, objects are skewed to the left for one camera and to the right for the other. (cf. *ibid.*) Viewed in the stereoscopic image, the objects seem to be leaning toward or backward depending on which camera images are left or right (Figure 63).

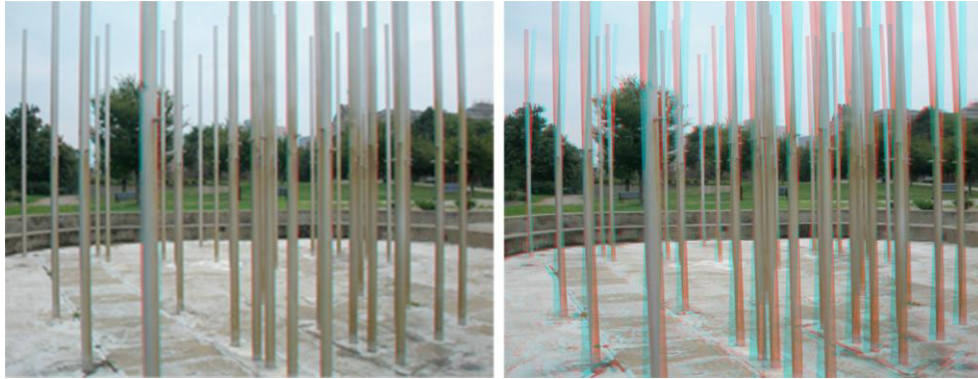


Figure 63: Dynamic scene including vertical lines.

Left: No rolling shutter. Right: Vertical lines skewed in opposite direction due to rolling shutter and beam-splitter.

5.1.3.2 Disparity of reflections

Stereoscopic 3D tries to simulate binocular vision to add depth to flat images by adding horizontal disparity.

In general, our visual system handles horizontal disparities very well – this is how we naturally see depth with binocular vision – by resolving horizontal differences in perspective. However, this effect can cause problems as the visual system cannot gather information through the small eye motion and head turning.

The viewer cannot reconcile an image, when features only appear to one eye or are significantly different to the left and right eye which is referred to as binocular rivalry (cf. chapter 3.2.1). This is frequently the case for reflections on surfaces that are not planar. Regarding a small interaxial distance and well synchronized cameras, reflections can usually be matched without problems.

The main reasons for reflections not matching on objects in the left and right image are the different positions and angles of the cameras and the view dependency of reflections, as demonstrated in Figure 64.

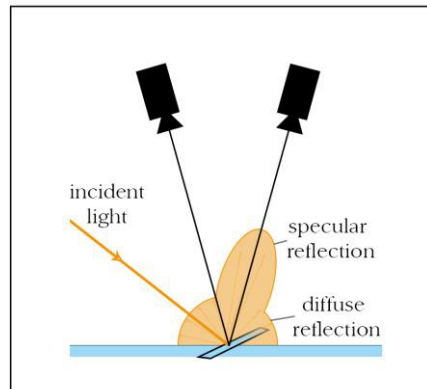


Figure 64: Different specular intensities on the two camera images.

Figure 65 shows the areas in a mapped stereo image where specular reflections and highlights provoke binocular rivalry. If the rivalries of the reflections are too large, it can be distracting for the viewer and challenging to correct in postproduction requiring advanced image processing. (cf. Stump, 2014)



Figure 65: Map of left and right image reflection difference.

Polarization filters can assist in avoiding reflections on non-metallic surfaces, as light is partially polarized on these surfaces.

5.1.3.3 Reflections and depth

Mirrors are often considered to be flat planes. However, regarding the shown reflections, this assumption is fundamentally wrong. When observing a mirror reflection, the visual system accommodates and converges as if it was true three-dimensional space. The reflection on the mirror, i.e. the virtual image referring to Figure 9, is located behind the mirror plane. Distance and parallax of the spatial mirror reflection have to be particularly considered and adjusted to the depth budget (cf. chapter 5.1.1).

A special case concerning depth is the appearance of lens flares in stereo 3D. Lens flares do not occur in binocular vision and there is no true depth of the lens flares as it is an artifact of internal lens reflections. Due to the lens flare's strong dependency on viewing position, the interaxial distance can cause mismatching. To create a pleasing depth composition of a lens flare, the flare can be launched at the far distance (with positive parallax) of a stereo scene, ideally at the light source it derives from, and be poked out towards the front (with negative parallax) of the scene. The flares' depth level needs to be adjusted to the depth budget of the scene.

5.1.4 Stereoscopic compositing

Stereoscopic movies have added a new turn to compositing. It requires two nearly identical composites for the left and right image which can cause breaks in convergence. One such issue that needs to be contemplated in stereo compositing is related to reflections and specular highlights. (cf. Okun et al., 2010, p. 569) If specular reflections or highlights strongly differ between the left and right image, they cannot be interpreted binocularly which leads to discomfort of the viewer. Thus, the reflections need to be conformed in the left and right channel in order to eliminate large disparity by isolating, i.e. rotoscoping, sometimes copying the reflection from the right image to the left image or vice versa and warping them.

In general, 2D compositing techniques can be applied in stereo compositing; however, for the right depth settings special consideration is required. When replacing green screen or integrating CG elements, the inserted elements must be positioned in the according depth level, otherwise the viewer cannot fuse in three-dimensional space.

Concerning the tracking of stereo scenes with fixed interaxial cameras, it is advisable to track one camera and then offset the other camera according to the interaxial distance and

convergence. If convergence varies across the shot or is unknown, a track for both cameras is required.

Applications such as Nuke, its plug-in Ocula to be exact, allow stereoscopic post-processing. Combining right and left composite trees in tandem enables separating the composite trees into a right and left branch and rejoining after the modifications. (cf. Okun et al., 2010, p. 569)

5.2 Light fields and reflective and transparent surfaces

5.2.1 Technology of light field camera

Light field describes a technique to capture a 4D light field (cf. Levoy et al., 1996), also called “Lumigraph” (cf. Gortler et al., 1996), instead of conventional 2D images. A light field contains additional spatial information, the intensity for each position (x, y) and the angular light direction (θ, ϕ) . The term light field was first described by Arun Gershun in 1936 in his paper defining the light field as radiance as a function of position and direction in free space, i.e. without occlusion. (cf. Gershun, 1939) In 1996, Levoy and Hanrahan introduced light fields into the computer graphic which allowed computing new perspectives from a scene of an existing view without a modeled 3D scene, which is referred to as image-based rendering. (cf. Levoy et al., 1996) Since then, a variety of theoretical and practical methods have been developed to improve transferring and capturing 4D radiance in terms of compatibility to flat images.

A light field can be considered as an array of images of a scene, each with a slightly different perspective from viewpoints located on a two-dimensional plane. If the viewpoints are close enough to each other and the views themselves wide-angled enough, the array contains information of the light leaving each point in the scene and traveling in every direction which is in fact the field of light surrounding the scene. Extracting pixels from these images allows constructing images for viewpoints besides the ones of the original array – with correct perspective and parallax.

There are different ways to capture such a light field:

- The simplest way is a single camera moving across a static scene capturing various perspectives, as demonstrated in Figure 66. For a static scene the different perspectives can be used to construct the light field.



Figure 66: To generate a light field of a static scene, a single moving camera capturing various perspectives is sufficient.

- A dynamic scene requires multiple cameras set up in an array to capture light fields (Figure 67).



Figure 67: Multi-camera array allows creating light field pictures for dynamic scenes.

Depending on the type of camera, the array can capture ultra-high speed video by staggering the triggering times of the cameras, high-resolution panoramas by spreading their angle of view or even HDR video by altering exposure times. (cf. Wilburn et al., 2005, p. 765–776)

- Another method – corresponding to the array of cameras but on the micro scale – is using an array of microscopic lenses (lenslets) with very small focal lengths. The array of lenslets is placed in front of the sensor in such a way that the main lens focuses on the lenslet array and the lenslet array on the sensor, which is the approach of the so called plenoptic camera. (cf. Ng et al., 2005)

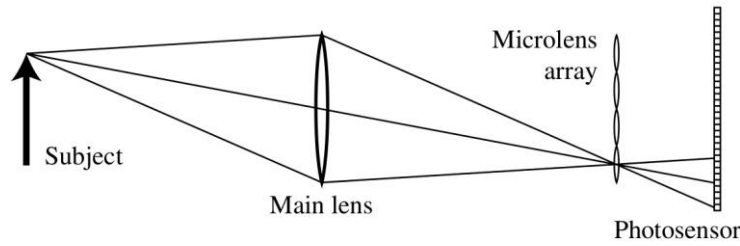


Figure 68: Simplified plenoptic camera model.

In Figure 68, light rays from a focused subject arrive on a lenslet which diverts the rays to different pixels on the sensor. This allows capturing the angular variation among the rays. However, as the sensor additionally captures angular information, the spatial resolution is reduced.

For all methods, the light fields can be interpreted computationally according to the following concept. Every sub-image of the array, no matter captured in which way of the above ones, differs slightly from its neighboring image. By finding matching light rays among all these images and their position in all the sub-images, the gathered information allows reconstructing a four-dimensional representation of the scene. To create any two-dimensional image within the given range of perspective the sampled rays from the 4D light field can be interpolated to generate the required rays for a certain view. The 4D light field can be considered as a collection of 2D images of a visual scene with the focal points of the different cameras or lenslets in another 2D plane. By stacking all views of the light field and taking only a (horizontal) slice of this stack, a 2D image results which is called epipolar plane image (EPI), as shown in Figure 69.

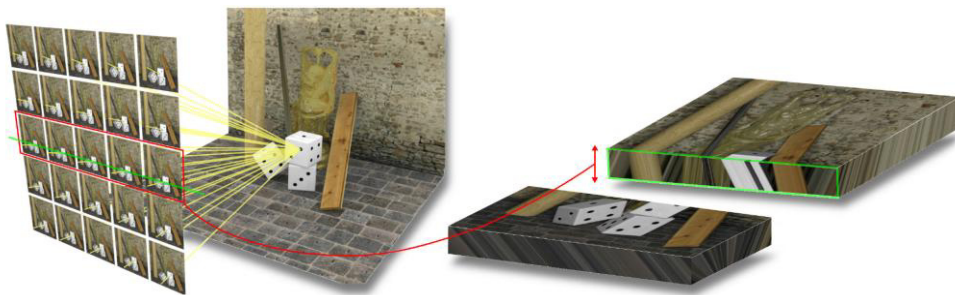


Figure 69: Stack of all images of the light field; cut (green box) through stack results in EPI.

4D light fields offer many possibilities over conventional flat images such as refocusing images (cf. *ibid.*), depth estimation (cf. Tao et al., 2013), (cf. Wanner et al., 2012), generating normal maps, change of focal length, relighting, change in perspective, to mention a few among many more.

Light fields further allow generating stereo images by combining two perspectives of the light field. It gives a maximum of flexibility and possibilities of adjusting interaxial distance, depth budget, disparity gradient, etc.

Furthermore, by either having a turntable or a gantry that circles around the object so that all horizontal perspectives of an object are captured in a light field, a model of the object can be generated. Therefore, light field techniques allow 3D scanning.

Another field of application of light fields is the implementation in 3D games by interactively rendering changing perspectives in real-time.

Since a few years, different consumer and industrial versions of light field cameras, i.e. Lytro and Raytrix, have made tremendous progress.

5.2.2 Problem of glossy surfaces and reflecting objects

Until recently, established algorithms to interpret the light field mostly detected corresponding patterns, assuming that an area looks the same in all sub-images.

By parallax calculation in the epipolar plane images, depth can be estimated. These algorithms, however, apply only for diffuse surfaces. Specular reflections and highlights, which by their nature slide over the surface, change shape and position in each different viewpoint, cause ambiguous information so that the matching of the corresponding areas fails which then leads to misleading depth values. As a result, changes of focus, perspective and focal length do not run smoothly for mirrorlike reflections, specularities or (semi) transparent surfaces.

Further, the interpolation algorithm for calculated views can make specular highlights become blurred or even disappear entirely.

5.2.3 Approach of solution

Depth estimation of specular surfaces and also specularities is a complex issue for algorithms. However, transparent and refractive surfaces are even more confounding for computational processing and hard to distinguish as surface with a depth level because transparent objects mostly inherit visual features of surrounding or background objects. As shown in the following sections, it requires more than one algorithm to handle different kinds of reflections.

5.2.3.1 Specular highlights

In 2014, Tao et al. released their approach to estimate both specular and diffuse, i.e. glossy surfaces. (cf. Tao et al., 2014)

The approach makes use of the property that specular highlights change with perspective and compares images of different viewpoints to detect highlights and then extract the specularities (Figure 70). Having a closer look at their algorithm, which is designed for the consumer light field camera Lytro, reveals that the algorithm might be adaptable to a light field sampled by a camera array.

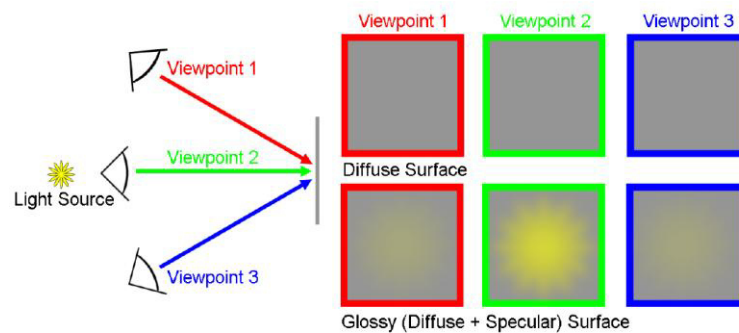


Figure 70: Extracting specular highlights due to viewpoint differences.

First, they estimate depth of the 4D light field image with diffuse and specular reflections. Then, using the light fields' ability of refocusing, the color of the light source and thus also the highlight color is analyzed by comparing different viewpoints in terms of color variance and brightness. (cf. *ibid.*, p. 2) Last, the highlights are extracted by using the given full 4D light field information and replacing the detected highlight areas with diffuse color information from other viewpoints, referring to Figure 70. (cf. *ibid.*) In the end, this specular-free image set is used to enhance the depth estimation. (cf. *ibid.*, p. 3)

5.2.3.2 Specular and transparent planes

The method of Tao et al. does not involve (semi) transparent surfaces. In general, there are two cases referring to the Fresnel equations that are unproblematic considering a plane surface: If the reflectance coefficient is (nearly) 1, the plane is a mirror and can be considered as a three-dimensional representation of the surrounding scene. Thus, while the surface is static, the light field “sees” a virtual three-dimensional space – like a window. If the transmission coefficient is approximately 1, then the plane is fully

transparent and thus does not have an effect on the estimate. All other values for the reflectance and transmission coefficients need closer consideration.

Wanner et al. published an approach to estimate depth of transparent and reflective surfaces by considering reflections and transparencies as overlaid line structures in planar EPI space with an orientation related to disparity. (cf. Wanner et al., 2013, p. 2) The slant of the lines indicates the structure of the scene. Using pattern analysis computation, the two layers of surface and reflection can be separated and the geometry of the partially reflective or transparent plane can be reconstructed. (cf. *ibid.*) With that approach, local estimations for the disparity of both layers can be computed. (cf. *ibid.*)

5.2.3.3 Refractive objects

Maeno et al. presented a method to detect transparent objects and analyze the refraction via a light field. As a refractive object shows more its surrounding background than revealing information about its own properties, it is difficult to extract its shape and position. Looking at a refractive object, it distorts the background elements. Maeno et al. aim to recognize transparencies by turning the background distortion to account. (cf. Maeno et al., 2013, p. 2788f) The distortion depends on the object's shape and index of refraction.

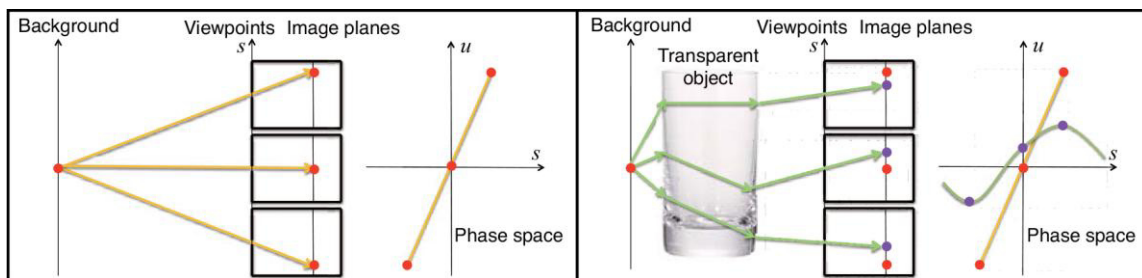


Figure 71: Light field transfer. Left: unbiased light field. Right: biased light field due to refraction.

Figure 71 shows the propagation of a light field in a simplified representation. On the left, light falls into the sensors of the camera array without an object between the cameras and the background element, i.e. no refraction and no reflection occurs. The rays from the background feature are straight, which results in constant disparity for the different viewpoints. The amount of disparity is an indicator of the distance between camera and background. (cf. *ibid.*)

Whereas with a transparent object between the background element and the camera array, on the right of Figure 71, the ray bends and changes its initial direction. Comparing

the features' locations in all viewpoints the representation of disparity gives a non-linear, ambiguous result. Maeno et al., however, do not offer an approach for further shape and position estimation.

Once a transparent region is detected, the most difficult part is still ahead. One approach could be by means of the Fresnel equations.

Usually for objects consisting of glass, total internal reflection occurs at the outline. For curved objects, i.e. convex or concave shape, the angle between the surface's normal and the viewpoint increases towards 90° . Total internal reflection occurs for glass-air interfaces at angles higher than the critical angle of approximately 42° which means that an algorithm can deduce an estimate of surface normals for parts where total internal reflection is detected in each viewpoint. Dark outlines, i.e. no light passing through, can be a hint for total internal reflection. White outlines can infer that reflections overlap total internal reflection at surface edges.

By analyzing the distorted image, for some areas of an object with basic shape, it might be possible to infer the refraction index that can then be assigned to parts of the object with more complex shape – supposing that an object with consistent material is observed.

Goal is to reconstruct the surface normals which then allow estimating shape and position of a transparent object. However, this approach only applies to basic concave or convex transparent object. For more complex shapes the algorithm fails. Several other cases have to be considered.

The visual system is able to interpret all kinds of different materials and shapes of transparent objects. However, computational algorithms struggle with assigning an object's characteristics of solely the appearance. The brain's interpretation of a scene benefits from experience, i.e. it knows by experience how different materials such as glass and liquids visually distort the background elements. Computational algorithms are based on commands and are not yet sophisticated enough to learn of given scenes. An approach for the future would be to establish an algorithm that accesses a data base of "experience", i.e. an algorithm that learns from each given situation and therefore improves the hit rate of interpreting a transparent object's shape, location and depth.

6 Conclusion and outlook

Reflections offer many benefits to the production of moving images. First, they add to an image's composition and create a visual enhancement. With the reflections' strong recognition value for material properties and their impact on depth estimation for the visual perception, reflections are an important component in a scene.

By using a beam-splitter, reflections offer possibilities for in-camera effects and thereby allow different perspectives at the same time. Some filming methods involving beam-splitters such as the Schüfftan process and front screen projection contributed to the development of visual effects. For other applications such as the stereoscopic filming method with a beam-splitter, reflections are essential and provide a high degree of flexibility. Specular reflections also simplify some procedures during film making such as creating light probe images by means of chrome ball reflections.

However, besides the great benefits, reflections pose a big challenge in various aspects. If specular reflections reveal undesired elements, they need to be retouched and therefore raise costs and time demand of the post-production. Further, inserting reflective CG objects into a live-action scene implies knowing the intrinsic behavior of reflections. The visual system intuitively distinguishes between diffuse and reflective surfaces and consciously or subconsciously recognizes incoherent reflections' behavior such as motion, intensity and compression. As reflections behave differently than diffuse textures, it requires well-founded knowledge in order to simulate realistic reflections and to seamlessly integrate them. Individual reflection studies may be needed to accomplish a pleasing result.

In addition, reflections can make match moving, stereo image adjusting and depth estimation in light fields extremely difficult. Especially for light field algorithms reflections and transparencies are very hard to handle. Therefore, it might have to be considered to eliminate reflections by using polarization filters, to entirely replace reflective objects, or to establish a new type of sophisticated algorithm simulating the visual system. In general, light field technique brings many advantages for filming methods. In the future, when computational algorithms are stable and effective enough, this technique can entirely replace the need of green screen. Mattes in any depth level of a scene could easily and reliably be created on demand owing to depth maps. Some state of the art processes related to reflections in film post-production would then certainly be redundant.

In summary, specular reflections and specular highlights require special consideration in nearly every captured scene. Everywhere, where there is light, there will be reflections.

Even if there are no reflective surfaces given in a scene, lens flares still are possible to occur.

Carefully considering and observing reflections in a live-action scene can avoid time-consuming and tedious post-production work. Even though specular reflections can be more of a nuisance in many aspects of production and post-production of moving images, they are indispensable for creating appealing images.

References

- Ahmed, Naveed; **BRDF Reconstruction from Video Streams of Multi-View Recordings**, University of Saarland, Saarbrücken, Germany, 2004.
- Aithadi, Nicolas; Larsen, Oystein; Pescosolido, Cristin; Wegerhoff, Frank; **Supervising a VFX shoot**, 3D WORLD, 06/2006.
- Allaby, Ailsa; Allaby, Michael; **Dictionary of Earth Sciences**, Oxford University Press, 1999.
- Artusi, Alessandro; Banterle, Francesco; Chetverikov, Dmitry; **A Survey of Specularity Removal Methods**, Computer Graphics Forum; vol. 20, no. 8; p. 2208–2230, 08/2011.
- Bell, David C.; **7 Surprisingly Low Budget Effects In Big Budget Movies**, Film School Rejects, 2013. <http://filmschoolrejects.com/cinematic-listology/7-surprisingly-low-budget-effects-in-big-budget-movies.php>, accessed 03.03.15.
- Birn, Jeremy; **Digital lighting & rendering**, 1st ed, New Riders, 2000.
- Birn, Jeremy; **Digital lighting & rendering**, 3rd ed., New Riders, 2014.
- Blake, Andrew; Bülthoff, Heinrich; **Does the brain know the physics of specular reflections?**, Nature; 343; p. 165–168, 1990.
- Center for Occupational Research and Development; **Geometric optics, Filters and Beam Splitters**, CORD Communications, 1987.
- Cock, Matthew; **Hitchcock's Blackmail and the British Museum: film, technology and magic**, British Museum, 2011. <http://blog.britishmuseum.org/2011/08/25/hitchcock%E2%80%99s-blackmail-and-the-british-museum-film-technology-and-magic/>, accessed 01.03.15.
- Dashwood, Tim; **A Beginner's Guide to Shooting Stereoscopic 3D**, Dashwood Cinema Solutions, 2011. <http://www.dashwood3d.com/blog/beginners-guide-to-shooting-stereoscopic-3d/>, accessed 01.03.15.
- Davidhazy, Andrew; **Front projection: a useful compositing special effects technique**, Rochester Institute of Technology, 2008.
- Debevec, Paul; **Image-Based Lighting**, IEEE Computer Graphics and Applications; 22 (2); p. 26–34, 04/2002.
- Dobbert, Tim; **Matchmoving: The Invisible Art of Camera Tracking**, 2nd ed., John Wiley & Sons, 2012.
- Fariss, Nathan; **Shooting and Assembling a High Dynamic Range Image (HDRI)**, Nathan Fariss film studios, 2011. <http://www.hello-napalm.com/tuts/hdri.html>, accessed 01.03.15.
- Fleming, Roland W.; Torralba, Antonio; Adelson, Edward H.; **Specular reflections and the perception of shape**, Journal of vision; 4(9), 10; p. 798–820, 09/2004.
- Gershun, Andrew; **The Light Field**, Journal of Mathematics and Physics; vol. 18; p. 51–151, 1939.
- Gortler, Steven J.; Grzeszczuk, Radek; Szeliski, Richard; Cohen, Michael F.; **The Lumigraph**, Computer Graphics (SIGGRAPH '96 Proceedings); p. 43–54, 1996.

- Hecht, Eugene; **Optics**, 4th ed., Addison-Wesley, 2002.
- Heeger, David; **Depth, Size, and Shape**, Department of Psychology, New York University, 2006.
- Howard, Ian P.; Rogers, Brian J.; **Perceiving in Depth, Stereoscopic Vision**, Volume 2, Oxford University Press, 2012.
- Kalloniatis, Michael; Luu, Charles; **The Organization of the Retina and Visual System**, Webvision, University of Utah, 2007.
- Kerrigan, Iona S.; Adams, Wendy J.; **Highlights, disparity, and perceived gloss with convex and concave surfaces**, Journal of vision; 13(1), 9, 01/2013.
- Knorr, Sebastian; **Basic rules for good 3D and avoidance of visual discomfort**, imcube 3, Berlin; p. 1–17, 9/2011.
- Koenderink, J. J.; van Doorn, A. J.; **Photometric Invariants Related to Solid Shape**, Optica Acta: International Journal of Optics; vol. 27, 7; p. 981–996, 1980.
- Levoy, Marc; Hanrahan, Pat; **Light Field Rendering**, Proceeding SIGGRAPH '96; p. 31–42, 1996.
- Levoy, Marc; Shade, Jonathan; **A light field of Michelangelo's statue of Night**, Stanford Computer Graphics Laboratory, 1999.
- Lightman, Herb A.; **Front Projection for "2001: A Space Odyssey"**, Schwam, Sabine (ed.), The Making of 2001: A Space Odyssey, 2000, Modern Library, New York, 1968.
- Lloyd, John; **A brief history of retroreflective sign face sheet materials**, Understanding retroreflectivity, REMA (Retroreflective Equipment Manufacturers Association); p. 1–4, 2008.
- Lvovsky, Alexander L.; **Fresnel equations**, Encyclopedia of Optical Engineering, Taylor & Francis, 2013.
- Maeno, Kazuki; Nagahara, Hajime; Shimada, Atsushi; Taniguchi, Rin-Ichiro; **Light Field Distortion Feature for Transparent Object Recognition**, Computer Vision and Pattern Recognition (CVPR); p. 2786–2793, 06/2013.
- Mendiburu, Bernard; Pupulin, Yves; Schklair, Steve; **3D TV and 3D Cinema: Tools and Processes for Creative Stereoscopy**, Focal Press, 2011.
- Minden, Michael; Bachmann, Holger; **Fritz Lang's Metropolis: Cinematic Visions of Technology and Fear**, Camden House, 2002.
- Murphy, Alexander A.; Fleming, Roland W.; Welchman, Andrew E.; **Key characteristics of specular stereo**, Journal of vision; 14 (14), 14, 12/2014.
- Murphy, Alexander A.; Welchman, Andrew E.; Blake, Andrew; Fleming, Roland W.; **Specular reflections and the estimation of shape from binocular disparity**, PNAS (Proceedings of the National Academy of Sciences of the United States of America); vol. 110, no. 6; p. 2413–2418, 02/2013.
- Myers, Rusty L.; **The Basics of Physics**, Greenwood Press, 2006.

- Nave, Carl R.; **Reflection**, 2012. <http://hyperphysics.phy-astr.gsu.edu/hbase/hframe.html>, accessed 01.03.15.
- Ng, Ren; Levoy, Marc; Brédif, Mathieu; Duval, Gene; Horowitz, Mark; Hanrahan, Pat; **Light Field Photography with a Hand-held Plenoptic Camera**, Stanford University Computer Science Tech Report CTSR 2005-02; p. 1–11, 04/2005.
- Nicodemus, F. E.; Richmond, J. C.; Hsia, J. J.; Ginsberg I. W.; Limperis, T.; **Geometrical Considerations and Nomenclature for Reflectance**, National Bureau of Standards, EG&G, Inc., Agro Science, Inc., Washington, D.C., Las Vegas, Nevada, Ann Arbor, Michigan, 1977.
- Novosad, Justin; **Render pass concepts and techniques**, Whitepaper, Autodesk, Inc., 2010.
- Okun, Jeffry A.; Zwerman, Susan; **The VES Handbook of Visual Effects, Industry Standard VFX Practices and Procedures**, 2nd ed., Focal Press, 2010.
- Perrine, J. O.; **Fermat's Principle of Least Time and Snell's Law of Refraction of Light**, School Science and Mathematics; vol. 61, issue 1; p. 5–14, 01/1961.
- Reeve, Simon; Flock, Jason; **Basic Principles of Stereoscopic 3D**, BSKYB Whitepaper, 2010.
- Ross, Brian J.; **Ray Tracing Basics**, Brock University, St. Catharines, Canada, 2014.
- Seymour, Mike; **The Art of Rendering**, FXguide, 2012. <http://www.fxguide.com/featured/the-art-of-rendering/>, accessed 03.03.15.
- Sfetcu, Nicolae; **The Art of Movies**, 1st ed., eBook, 2011.
- Stallings, Billee J.; Evans, Jo-an J.; **Murray Leinster: The Life and Works**, McFarland, 2011.
- Stump, David; **The Basics of Stereo Photography**, ASC, 2014.
http://64.17.134.112/Affonso_Beato/The_Basics_of_Stereo_Photography.html, accessed 14.02.15.
- Tan, Ping; Lin, Stephen; Quan, Long; Shum, Heung-Yeung; **Highlight Removal by Illumination-Constrained Inpainting**, Computer Vision; vol. 1; p. 164–169, 08/2003.
- Tao, Michael; Hadap, Sunil; Malik, Jitendra; Ramamoorthi, Ravi; **Depth from Combining Defocus and Correspondence Using Light-Field Cameras**, University of California, Berkley, 2013.
- Tao, Michael; Wang, Ting-Chun; Malik, Jitendra; Ramamoorthi, Ravi; **Depth Estimation for Glossy Surfaces with Light-Field Cameras**, University of California, Berkeley; University of California, San Diego, 2014.
- Tauer, Holger; **Stereo-3D, Grundlagen, Technik und Bildgestaltung**, Schiele & Schön, 2010.
- Templin, Krzysztof; Didyk, Piotr; Ritschel, Tobias; Myszkowski, Karol; Seidel, Hans-Peter; **Highlight microdisparity for improved gloss depiction**, ACM Transactions on Graphics (Proceeding SIGGRAPH 2012); 31, 4, 92; p. 1–5, 07/2012.
- Thompson, William; Fleming, Roland W.; Creem-Regehr, Sarah; Stefanucci, Jeanine K.; **Visual perception from a Computer Graphics Perspective**, A K Peters, 2011.

- Wanner, Sven; Goldluecke, Bastian; **Globally Consistent Depth Labeling of 4D Light Fields**, Heidelberg Collaboratory for Image Processing, 2012.
- Wanner, Sven; Goldluecke, Bastian; **Reconstructing Reflective and Transparent Surfaces from Epipolar Plane Images**, Heidelberg Collaboratory for Image Processing, 2013.
- Wendt, Gunnar; Faul, Franz; Mausfeld, Rainer; **Highlight disparity contributes to the authenticity and strength of perceived glossiness**, Journal of vision; vol. 8, no. 1, 14, 01/2008.
- Wilburn, B.; Joshi, N.; Vaish, V.; Talvala, E.-V.; Antunez, E.; Barth, A.; Adams, A.; Horowitz, M.; Levoy, M.; **High Performance Imaging Using Large Camera Arrays**, Electrical Engineering Departement, Stanford University, 2005.
- Witte, Kirk; **How to shoot a chrome ball for HDRI**, Savannah College of Art & Design, 2007.
- Wright, Steve; **Digital compositing for film and video**, 3rd ed., Elsevier/Focal Press, 2010.
- Wright, Steve; **Parallel vs Converged**, Digital FX, 2011.
http://vfxio.com/PDFs/Parallel_vs_Converged.pdf, accessed 02.03.15.
- Wynn, Chris; **An Introduction to BRDF-Based Lighting**, NVIDIA Corporation; p. 1–90, 2000.
- Zhi, Jin; **A process of seamlessly replacing CG elements into live-action footage**, Duncan of Jordanstone College of Art & Design, United Kingdom, 2013.
- Zisserman, Andrew; Giblin, Peter; Blake, Andrew; **The information available to a moving observer from specularities**, Image and vision computing; vol. 7, issue 1; p. 38–42, 02/1989.

List and References of Figures

Figure 1: Light interacting with matter.	6
Figure 2: Proof of Fermat's principle of reflection. (cf. Nave, 2012)	7
Figure 3: The law of refraction. (cf. © 2006 Encyclopædia Britannica, Inc.)	9
Figure 4: Parallel (p-) and perpendicular (s-) polarization to the plane of incidence. (© 2005 Japan Atomic Energy Research Institute)	10
Figure 5: Left: Reflectance R_s and R_p at an air-glass interface. Right: Brewster's Angle. (© 2015 stack exchange, Inc)	11
Figure 6: Left: R_s and R_p at a glass-air interface. Right: Critical angle and total internal reflection. (© 2015 stack exchange, Inc), (Nave, 2012)	12
Figure 7: Types of reflection.	13
Figure 8: Materials have different reflectance properties.	14
Figure 9: The virtual image appears to be the same distance behind the specular surface as the object is in front of it.	15
Figure 10: Anisotropic reflections on hair and brushed metal.	16
Figure 11: The surface of a reflective object changes utterly when varied in position. (Fleming et al., 2004)	17
Figure 12: Recovering shape by analyzing the distortion.	18
Figure 13: Surface perception changes when intensity of highlights changes. (Tan et al., 2003), (Artusi et al., 2011)	19
Figure 14: Comparison of a textured surface on the left column and a mirror on the right. (Fleming et al., 2004)	20
Figure 15: There is no compression of the reflection when a planar mirrorlike surface is rotated away from the viewer. (ibid.)	20
Figure 16: A sphere stretched to an egg shape – with textured surface in the left column and mirror surface in the right column. (ibid.)	21
Figure 17: The more curved the surface, the higher the range of reflection. (ibid.)	21
Figure 18: a_L and a_R as well as b_L and b_R are corresponding retinal points. (Kalloniatis et al., 2007)	23
Figure 19: While the grey dot is the eyes' fixation point, A and B stimulate non-corresponding retinal points leading to double vision. (ibid.)	23
Figure 20: Panum's fusional area spreads around the horopter including fixation point.	24
Figure 21: Horizontal grating presented to one eye continuously changing to vertical grating perceived by the other eye. (Heeger, 2006)	24
Figure 22: Specularities lie behind convex surfaces (left), but in front of concave surfaces (right). (cf. Templin et al., 2012)	25
Figure 23: Disparity of highlight position in binocular vision. (Murty et al., 2013)	26
Figure 24: Front projection technique. (Davidhazy, 2008)	28
Figure 25: Glass beads retro-reflecting light rays.	30

Figure 26: Beam-splitter cube, which can be polarizing or non-polarizing. (© 2014 Edmund Optics Inc.)	31
Figure 27: Front screen projection in the "Dawn of Man" scene. (Kubrick, Stanley; 2001: A Space Odyssey, Stanley Kubrick Productions/Warner Bros., 1968)	31
Figure 28: Introvision used in the train crash scene in "The Fugitive". (Davis, Andrew; The Fugitive, Warner Bros., 1993)	32
Figure 29: Schüfftan process applied in scene from Fritz Lang's "Metropolis". (© 2015 The Hitchcock Zone)	33
Figure 30: Producing the road scene in Metropolis via stop motion. (© 1999-2015 Getty Images, Inc.)	34
Figure 31: Actors seemingly on the roof of the British Museum in Hitchcock's "Blackmail". (Hitchcock, Alfred; Blackmail, StudioCanal Films, 1929)	34
Figure 32: Alfred Hitchcock using the Schüfftan Process in "The 39 Steps". (© 2015 The Hitchcock Zone)	35
Figure 33: Applying the Schüfftan process in "Lord of the Rings". (© 1999-2013 TheOneRing.net), (www.herr-der-ringe-film.de), (Jackson, Peter; The Lord of the Rings: The Return of the King, New Line Cinema, 2003)	35
Figure 34: High-angle shot realized with a mirror.	36
Figure 35: Realization of space jump scene in "Star Trek", 2009.	36
Figure 36: Creating the "Mirror Man" by using a life-size reference. (© 2012 Universal Studios), (Sanders, Rupert; Snow White and the Huntsman, Universal Studios, 2012)	37
Figure 37: Reflections and refraction give rendered scenes a more realistic impression. (Birn, 2000), (Birn, 2014)	38
Figure 38: Realizing the mirror room scene in "Divergent". (© 2014 Summit Entertainment)	41
Figure 39: Virtual camera located behind the mirror to capture the reflection image.	42
Figure 40: Visual simplification of the bidirectional functions.	43
Figure 41: The BDRF's parameters with radiance of the incident beam L_i (green) and the radiance of the reflected beam L_r (red). (© 2010 The National Institute of Standards and Technology (NIST))	44
Figure 42: Conservation of Energy. The quantity of reflected and absorbed light must be equal to the quantity of incoming light.	45
Figure 43: Changing appearance with different anisotropy values. Left: anisotropy = 1.0, center: anisotropy = 4.0, right: anisotropy = 8.0. (© 2015 Autodesk Inc.)	46
Figure 44: The reflectance of the specular floor varies with the viewing angle. (© 2015 Autodesk Inc.)	46
Figure 45: High ratio of transmittance (left), high ratio of reflectance (right), according to Fresnel equations. (Birn, 2000)	47
Figure 46: Specular map of a face.	47
Figure 47: Exposure bracketing and final HDR.	48
Figure 48: High dynamic range image. (© 2011-2014 CGTrader)	49
Figure 49: Chrome ball captures do not cover a 360 degree panorama. (Fariss, 2011)	50
Figure 50: A small reflection of the camera itself will be easy to remove. (Witte, 2007)	50

Figure 51: Image-based lighting with a light probe image mapped on a sphere. (© 2015 Atlassian)	51
Figure 52: Basic ray-tracing method. (© 2015 The University of Southern California)	52
Figure 53: Ray-tracing modeling and light paths. (© 2009 Visualization Sciences Group SAS.)	53
Figure 54: The number of reflections increases with ray depth. (by using Figure 48)	53
Figure 55: Caustic arising from sun light reflecting off a mug's curved inside.	54
Figure 56: Combining different render passes to a final composite. (© 2013 Pixel D Studios)	57
Figure 57: The impact of interaxial distance on the perception of depth. (Reeve et al., 2010)	61
Figure 58: An object's position in relation to the screen is determined by the convergence point. (ibid.)	61
Figure 59: Positive parallax for more distant objects (green line), negative parallax for closer objects (orange line). (ibid.)	62
Figure 60: Left: side-by-side rig, right: beam-splitter rig. (Dashwood, 2011), (© 2014 3ality Technica)	63
Figure 61: Different constructions to direct the two images with mirrors. (Tauer, 2010)	63
Figure 62: Standard beam-splitter rig. (Tauer, 2010)	64
Figure 63: Dynamic scene including vertical lines. (Stump, 2014)	66
Figure 64: Different specular intensities on the two camera images.	67
Figure 65: Map of left and right image reflection difference. (Stump, 2014)	67
Figure 66: To generate a light field of a static scene, a single moving camera capturing various perspectives is sufficient. (Levoy et al., 1999)	70
Figure 67: Multi-camera array allows creating light field pictures for dynamic scenes. (© 2014 Lytro, Inc.)	70
Figure 68: Simplified plenoptic camera model. (Ng et al., 2005)	71
Figure 69: Stack of all images of the light field; cut (green box) through stack results in EPI. (Wanner et al., 2012)	71
Figure 70: Extracting specular highlights due to viewpoint differences. (Tao et al., 2014)	73
Figure 71: Light field transfer. Left: unbiased light field. Right: biased light field due to refraction. (Maeno et al., 2013)	74